International Atomic Energy Agency

INDC(CCP)-295/L

INDC

INTERNATIONAL NUCLEAR DATA COMMITTEE

EVALUATED NUCLEAR CONSTANTS FOR URANIUM-236
(Preprint No. 2)

A.B. Klepatskij, V.A. Kon'shin, V.M. Maslov,
Yu.V. Porodzinskij, E.Sh. Sukhovitskij
Byelorussian SSR Academy of Sciences
Institute of Nuclear Power Engineering
Minsk, USSR

Translated by the IAEA

January 1989

IAEA NUCLEAR DATA SECTION, WAGRAMERSTRASSE 5, A-1400 VIENNA

INDC(CCP)-295/L

EVALUATED NUCLEAR CONSTANTS FOR URANIUM-236
(Preprint No. 2)

A.B. Klepatskij, V.A. Kon'shin, V.M. Maslov,
Yu.V. Porodzinskij, E.Sh. Sukhovitskij
Byelorussian SSR Academy of Sciences
Institute of Nuclear Power Engineering
Minsk, USSR

Translated by the IAEA

January 1989

Reproduced by the IAEA in Austria
January 1989

89-00155

EVALUATED NUCLEAR CONSTANTS FOR URANIUM-236

Preprint No. 2

A.B. Klepatskij, V.A. Kon'shin, V.M. Maslov,
Yu.V. Porodzinskij, E.Sh. Sukhovitskij

Byelorussian SSR Academy of Sciences
Institute of Nuclear Power Engineering
Minsk

ABSTRACT

New results are presented for the evaluation of the data for neutron interaction with ^{236}U. A complete system is given for evaluated neutron data in the neutron energy range 10^{-5}-20 MeV, established using up-to-date theoretical models. Application of the coupled-channel method and of a statistical model with correct calculation of the transmission coefficients and level density of nuclei, together with the use of new experimental data, have made it possible to enhance the reliability of neutron cross-section evaluation for ^{236}U.

INTRODUCTION

The need for a more accurate knowledge of the nuclear data for ^{236}U ensues from the fact that, in the re-use of spent uranium (regenerated material), the nuclear fuel registers a substantial increase in the content of ^{236}U, which is a poison and impairs the utilization of neutrons in a reactor [1]. In order to offset the effect of ^{236}U in regenerated fuel it is necessary to increase the initial ^{235}U concentration. This depends on the amount of ^{236}U in the regenerated material and on fuel element design. As pointed out in Ref.[2], two problems arise during the reprocessing of irradiated uranium fuel: the ^{232}U content and the high concentration of ^{236}U in the reprocessed uranium. An appreciable quantity of ^{236}U is accumulated in the fuel (approximately 0.5%), while the residual enrichment of the fuel in ^{235}U is less than 1% (in WWER-type reactors). Hence, during reactor operation it is necessary to take account of the effect of reactivity from ^{236}U [3]. Furthermore, ^{236}U is the source of ^{232}U formation in the fuel, along with the ^{238}U (n,2n) process, since after the (n,γ) process ^{236}U is converted into ^{237}U, and

$$U^{237} \xrightarrow{\beta^-(6,75\ d)} {}^{237}Np \xrightarrow{(n,2n)} {}^{236}Pu \xrightarrow{\alpha\ (2,85y)} {}^{232}U .$$

This situation evokes the need to evaluate the neutron cross-sections for ^{236}U. Application of the coupled-channel method and of a statistical model of the nucleus with correct calculation of the neutron transmission coefficients and level density parameters, and also the employment of new experimental data, have made it possible to increase the reliability of evaluations of the neutron cross-sections for ^{236}U. The table gives the values of energies for Q and thresholds T [4, 5] for various neutron reactions with the ^{236}U nucleus, linked by the relationship

$$T = \frac{M_n + M_{236}}{M_{236}} \cdot (-Q) = \frac{1,0086652 + 236,0455820}{236,0455820} \cdot (-Q) =$$

$$= 1,00427\,(-Q)\,.$$

Values of energies Q and thresholds T for reactions of neutrons with the $^{236}_{92}U$ nucleus

Reaction	Q, MeV	T, Mev	Reaction	Q, MeV	T, MeV
(n,γ)	–	– 5,I2	(n, t)	– 4,800	4,82
(n,2n)	– 6,546	6,57	(n, nt)	– 9,997	I0,04
(n,3n)	– II,85I	II,90	(n, ^{3}He)	– 5,048	5,07
(n,4n)	– I8,692	I8,77	(n, n^{3}He)	– II,222	II,27
(n,p)	– 2,320	2,33	(n, ^{4}He)	9,320	– 9,36
(n,np)	– 7,I60	7,I9	(n, n^{4}He)	4,55I	– 4,57
(n,d)	– 4,939	4,96			
(n,nd)	– II,053	II,I0			

The ground state of ^{236}U has spin and parity 0^+. The level diagram for ^{236}U has been studied in detail up to 1400 keV. The half-life of ^{236}U is 2342 x 10^7 years for alpha decay, and (2.7 ± 0.4) x 10^{16} years for spontaneous fission [6].

1. NEUTRON CROSS-SECTIONS IN THE RESOLVED RESONANCE ENERGY RANGE 10^{-5} eV-1 keV

Most of the experimental data on cross-sections in the resolved resonance energy range is inaccessible in numerical form. Hence evaluation of the cross-sections has been carried out on the basis of the resonance parameter values quoted in the original studies. This approach to the problem in general reduces the reliability of the results obtained, but for the specific nucleus ^{236}U it would appear to be sufficiently reliable in view of the simplicity of the analysis involved, since $\langle D \rangle > 10$ eV, and $\sigma_f \ll \sigma_t$

and σ_{γ} for all resonances. The parameters of the negative and first resonances can be further refined from measurements of the cross-sections at the thermal point (0.0253 eV).

1.1. Experimental work on determination of resonance parameters in the resolved resonance energy region

In carrying out the evaluation, use was made of the following measurements in the resolved resonance energy region:

1. Harvey and Hughes [7] measured the total cross-section σ_t over the energy range 2.75-700 eV with insufficiently high resolution, which yielded the resonance parameters only up to 378 eV.

2. Carraro and Brusegan [8] determined the total cross-section in the energy range 40 eV-4.1 keV. The parameters for 185 resonances were determined.

3. Mewisson, et al., [9] measured σ_t, $\sigma_{n\gamma}$ and σ_n in the energy range 30 eV-1.8 keV, Γn for 97 levels and $\Gamma\gamma$ for 57 resonances.

4. Carlson, et al., [10] determined the capture cross-section $\sigma_{n\gamma}$ up to energies of 20 keV. The resonance parameters were derived up to 415 eV.

5. Harlan [11] measured the total cross-section in the energy range 0.01-1000 eV. He reported preliminary resonance parameter values up to 376 eV.

6. McCallum [12] determined the total cross-section in the first resonance region.

7. Theobald, et al., [13] measured the fission cross-section and obtained a value for Γ_f in the region up to 415 eV.

The resonance parameter values obtained in the above studies are given in Tables 1.1, 1.2 and 1.3. At the thermal point (0.0253 eV) measurements were made of the absorption cross-section σ_a [10, 14-17], and the total cross-section σ_t [12] (Table 1.2). Table 1.3 gives the experimental values for capture resonance integrals [14-17].

1.2. Evaluated resonance parameters

As can be seen from Table 1.1, the experimental values for the resonance parameters are essentially not at variance with one another, although the precise location of the resonances is determined in a rather arbitrary manner. Hence, in the first instance the resonance parameters were evaluated, with the exception of the negative and first resonances, since their values were refined on the basis of the cross-sections, at the thermal point and in the region of the first resonance. The resonance energies in our evaluation up to 415 eV were taken basically from Ref. [10], since the measurements in the latter were conducted at lower energies and over a wider energy range (up to 20 keV). In addition, in experiments on radiative capture measurement the location of resonances is determined more accurately than in the measurement of total cross-sections, where the position of the resonance peaks is affected by interference from potential and resonance scattering. Above 415 eV the resonance energies were based on those in Refs [8, 9], performed on one and the same experimental facility and having the same energy scale.

The resonance neutron widths were derived by averaging, taking account of the errors in the experimental results from the studies in which total cross-section was measured.

The radiation widths given in the studies in which $\sigma_{n\gamma}$ was measured were overdetermined using evaluated neutron widths in such a way that the area below each of the capture resonances was retained, i.e. $\frac{\Gamma\gamma_i \, \Gamma n_i}{\Gamma_i}$. Then the radiation widths were averaged, as in the case of Γ_{ni}, with corresponding errors.

The fission widths were taken from Ref. [13] for those resonances in which they were measured. Since experiment did not reveal the fission cross-section structure which would be expected in the case of sub-barrier fission, the fission widths for the other resonances were assumed to be equal to the mean values from Ref. [13]. The first resonance energy and widths were also determined in accordance with the above-described procedure. They were then varied within the limits of error so as to describe, taking account of the negative resonance, the experimental data in the region before the first resonance and the figure, evaluated by us, for the radiative capture cross-section at 0.0253 eV, i.e. $5.0 \times 10^{-28} m^2$. The evaluated resonance parameters are given in Table 1.1.

1.3. Evaluated cross-sections in the resolved resonance region

The evaluated neutron cross-sections in the resolved resonance region from 10^{-5} eV to 1 keV were calculated in accordance with the Breit-Wigner multilevel formula, using the evaluated resonance parameters as in Table 1.1:

$$\sigma_n(E) = 4\pi R^2 + \sum_i \left[4\pi \lambda^2 \left(\frac{E}{E_{oi}}\right) \left(\frac{\Gamma_{ni}}{\Gamma_i}\right)^2 \frac{1}{1+x^2} + 2\sqrt{4\pi\lambda^2} \times \right.$$

$$\left. \sqrt{4\pi R^2} \left(\frac{E}{E_{oi}}\right)^{1/2} \frac{\Gamma_{ni}}{\Gamma_i} \frac{x}{1+x^2} \right];$$

$$\sigma_{\gamma,f}(E) = 4\pi\lambda^2 \sum_i \frac{\Gamma_{ni}\Gamma_{\gamma,fi}}{\Gamma_i^2} \left(\frac{E}{E_{oi}}\right)^{1/2} \frac{1}{1+x^2},$$

where $4\pi\lambda^2 = \left(\frac{A+1}{A}\right)^2 \frac{K}{E}$; A is the mass number; $K = 2.60382 \times 10^{-22} m^2 \cdot eV$; $\Gamma_i = \Gamma n_i + \Gamma\gamma_i + \Gamma f_i$; E_{oi} is the energy of the i-th resonance; $x = 2\frac{E-E_{oi}}{\Gamma}$; $4\pi R^2 = 11.4 \cdot 10^{-28} m^2$ is the evaluated potential scattering cross-section, derived on the basis of calculations employing the coupled-channel method and of concordance with the measured values of σ_t in the thermal region.

The evaluated cross-sections at the thermal point are:
$\sigma_t = (18.58 \pm 1.50) \times 10^{-28} m^2$, $\sigma_n = (13.51 \pm 1.00) \times 10^{-28} m^2$,
$\sigma_{n\gamma} = (5.00 \pm 0.14) \times 10^{-28} m^2$, $\sigma_f = (0.07 \pm 0.03) \times 10^{-28} m^2$.
The capture resonance integral for E = 0.5–1000 eV, calculated in accordance with evaluated figures for the parameters, is $323.4 \times 10^{-28} m^2$.

For convenience, Tables 1.4 and 1.5 quote the evaluated cross-sections in the range 10^{-5}–10 eV disregarding Doppler broadening and at room temperature (293 K).

1.4. Evaluated mean parameters from data in the resolved resonance energy region

In the region up to 1132.1 eV 72 resonances were experimentally established, giving $\langle D \rangle_{obs} \simeq 15.87$ eV and the mean reduced neutron width $\langle \Gamma_n^o \rangle = 1.88\ (meV)^{1/2}$. These values must be corrected for the omission of levels owing to the smallness of the neutron widths and the presence of multiplets. These omissions were allowed for using the method proposed in Ref. [18]. The methods of introducing corrections for omissions of levels described in the literature are based on use of the Porter-Thomas distribution for neutron widths. The originators, in one way or another, determine the Porter-Thomas distribution as "distorted" through the omission of levels. The distribution of the level spacings is not made use of, and no attempt is made to determine a "distorted" Wigner distribution. Simultaneous use of these two distributions is made in the method described in Ref. [18], which is based on a proposed model probability function for omission of levels, leading to distortion of the theoretical neutron width and level spacing distributions. Then a comparison of the theoretical and experimental distributions by the maximum likelihood method was used to determine the parameters of the model probability function for omission of levels and, consequently, the mean neutron widths and level spacings. It was assumed that all the resonances observed are s-levels and therefore the p-resonances were ignored. It seems to us that consideration of both distributions (Porter-Thomas and Wigner) makes it possible more accurately to make allowance for the experimental conditions and more accurately to make corrections for level omission. Calculations performed by this method have shown that the mean level spacings <D> are about 10% lower than those derived by other methods. Application of the method described in Ref. [18] showed that in the region up to 1132.1 eV approximately 12% of levels are omitted, and that allowing for the omission of levels the values $<\Gamma_n^o>$ and <D> are 1.634 $(MeV)^{1/2}$ and 14.13 eV.

The number of fission widths measured was too small for determining the statistical qualities of the selection, and therefore the mean value $<\Gamma_f>$, equal to the experimental value, was taken for this purpose. The mean radiation width $<\Gamma_\gamma>$ was derived by direct averaging of the evaluated quantities Γ_γ, since on the assumption that the distribution of the experimental radiation widths is subject to a χ^2 distribution, the number of degrees of freedom

$$\nu_\gamma = \frac{2 < \Gamma_\gamma >^2}{< \Gamma_\gamma^2 > - < \Gamma_\gamma >^2}$$

was equal to $\nu_\gamma \sim 40$.

Thus, assuming the presence of only s-resonances, the evaluated mean resonance parameters are:

$$<D> = 14,1 \pm 0,5 \ eV;$$
$$<\Gamma_n^o> = 1,63 \pm 0,25 \ (Mev)^{1/2};$$
$$<S>_o = (1,16 \pm 0,18)\cdot 10^{-4} \ (eV)^{-1/2};$$
$$<\Gamma_\gamma> = 22,77 \pm 1,30 \ MeV;$$
$$<\Gamma_f> = 0,354 \pm 0,100 \ MeV.$$

The reduced errors <D>, $<\Gamma_n^o>$, $<\Gamma_f>$ and $<S>_o$ are essentially statistical, determined by the finiteness of the selection; the error $<\Gamma_\gamma>$ is essentially systematic, associated with the normalization of $\sigma_{n\gamma}$. The evaluated quantity $<D>_{ev}$ is substantially lower than the values (16.2 ± 0.8) eV [1], (16.1 ± 0.5) eV [3] and 16.2 eV [4]. Allowing for the corrections introduced by the authors for the omission of weak levels, the values for <D> are respectively (16.2 ± 0.8) eV, (15.2 ± 0.5) eV and $(15.4 {}^{+2.2}_{-1.0})$ eV, and within the limits of error are in agreement with our evaluation, although the latter is lower. The given evaluation <D> is preferable, since upon introduction of a correction for level omission on the basis of the method described in Ref. [18], it takes simultaneous account of data for two experimental distributions: level spacing and neutron widths. The evaluated quantity $<\Gamma_n^o>$ virtually coincides with the quantities derived in Refs [8-10], while the difference in $<S>_o = \frac{<\Gamma_n^o>}{<D>}$ is determined by non-coincidence with <D>. The evaluation $<\Gamma_\gamma>_{ev}$ practically coincides with the values (23.0 ± 1.5) MeV [9] and agrees with the result (23. ± 1.0) MeV of Ref. [10].

2. NEUTRON CROSS-SECTIONS IN THE UNRESOLVED RESONANCE ENERGY RANGE 1-150 keV

The unresolved resonance region was considered at energies of from 1-150 keV. The lower limit was determined by the dimensions of the experimentally resolved resonance region. At the upper end, the limitations are associated above all with ignorance of the value of the strength function S_2 and the presence of a second level (149.48 keV, 4^+).

In deriving evaluated data for unresolved resonance energies, allowance was made for the contribution of s-, p- and d-waves. Allowance for the d-wave contribution is associated with the nature of the non-fissioning nucleus, since owing to the absence of fission competition capture of d-wave neutrons constitutes a considerable part of the radiative capture cross-section. The extent of the energy region made it necessary to take account of the energy dependence of the mean level spacings and of radiation widths.

2.1. Experimental data on ^{236}U cross-sections in the unresolved resonance energy range

In the unresolved resonance region, measurements have been made only of the radiative capture cross-section:

1. Carlson, et al., [10] determined $\sigma_{n\gamma}$ in the region up to 20 keV (Table 2.1);

2. Bergman, et al., [19] measured the cross-sections $\sigma_{n\gamma}$ in the 0.1-5 keV range (Table 2.2);

3. Kazakov, et al., [20] determined the mean capture cross-sections at intervals for energies in the 3-420 keV range (Table 2.3);

4. Grudzevich, et al., [21, 22] measured $\sigma_{n\gamma}$ in the range 0.15-1.1 MeV (Table 2.4);

5. Muradyan, et al., [72] measured $\sigma_{n\gamma}$ in the range 0.4-80 keV and 0.2-1.6 MeV using a "multiplicity" spectrometer.

In addition, the experimental data on fission cross-section in the unresolved resonance region include one point taken from Ref. [23] at 127 keV ($\sigma_f(^6U)/\sigma_f(^5U)$ = 0.0012 $\pm$ 0.0006) and an upper limit for σ_f of 4.0 x $10^{-31} m^2$ at 24 keV, measured in Ref. [24].

2.2. Evaluated mean resonance parameters in the 1-150 keV range

For deriving the mean parameters use was made of the method recommended in the ENDF/B format.

The mean-level spacings $\langle D\rangle_J$ of spin J were determined from $\langle D\rangle_{ev}$ in the resolved resonance energy region, using the level density from the superfluid nucleus model taking account of the vibrational and rotational modes [25, 26]. The parameters of the model are described in detail in section 5.2. The evaluated mean level spacings $\langle D\rangle_J$ for the ^{237}U nucleus are given in Table 2.5. (The model omits dependence of $\langle D\rangle_J$ on parity.)

The mean neutron widths were calculated via the strength functions S_ℓ^{0+} for the ground state

$$\langle \Gamma_n\rangle_J^\ell = S_\ell^{0+}\langle D\rangle_J E^{1/2} P_\ell ,$$

where P_ℓ = transmission coefficients of the partial wave ℓ, calculated with reference to the "black" nucleus model.

This "black" nucleus model was used only for determining the transmission coefficients of the nuclear surface in a narrow energy range (up to 150 keV). The strength functions S_0 and S_1 were calculated by the coupled-channel method. Hence the non-correctness of the model had practically no effect on the final results, particularly since the results of calculating the transmission coefficients for s- and p-neutrons by the coupled channel method and the "black" nucleus model agree with each other within limits of < 5% and more up to energies of 200 keV.

The strength function S_0^{0+} in the ground state is taken as equal to that evaluated from the resolved resonance region $S_0^{0+} = 1.156 \times 10^{-4} (eV)^{-1/2}$, and strength function $S_1^{0+} = 1.74 \times 10^{-4} (eV)^{-1/2}$ calculated from a generalized optical model with potential parameters, whose choice is described in section 4.2. With calculations using the coupled-channel method and selected potential parameters the value $S_0^{0+} = 1.164 \times 10^{-4} (eV)^{-1/2}$ is derived. The strength functions S_2, according to Dresner [27], are taken as equal to S_0. The evaluated mean neutron widths are given in Table 2.6.

The mean neutron inelastic widths $\langle\Gamma_{n'}\rangle_{J\pi}$ are determined according to the formula

$$\langle\Gamma_{n'}\rangle_{J\pi} = \langle D\rangle_J \sum_{\ell'} S_{\ell'}^{2^+} \varepsilon_q^{1/2} P_{\ell'}(\varepsilon_q)\, \nu_{J\ell'} \quad ,$$

where $\varepsilon_q = (E - E_q)$ is the neutron energy after scattering in the inelastic channel with energy E_q (in the unresolved resonance energy region only one level 2^+ ($E_q = 45.24$ keV) is excited); $\nu_{J\ell'}$ is the number of degrees of freedom for the given state.

The calculations make allowance for the various strength function values for the ground S^{0+} and excited S^{2+} states, reckoned on the basis of a generalized optical model [28]:
The evaluated figures $\langle\Gamma_{n'}\rangle_{J\pi}$ are given in Table 2.7.

The authors of Ref. [13] found no resonance structure in the fissioning widths of resolved resonances for ^{236}U, which may be explained by the presence of levels in the second well of the fission barrier. Hence in the unresolved resonance region the mean fission widths $\langle\Gamma_f\rangle$ were calculated to a one-hump approximation according to the Hill-Wheeler model:

$$\langle\Gamma_f\rangle_{J\pi} = \frac{\langle D\rangle_J}{2\pi}\, \nu_f \frac{1}{1 + \exp\left[\dfrac{2\pi(E_f^{J\pi} - E)}{\hbar\omega}\right]} \quad .$$

The fission barrier parameters in the $1/2^+$ channel were so selected as to ensure that the calculated average fission width $\langle\Gamma_f\rangle_{1/2+}$ $(E = 0)$ was equal to the mean value from the resolved resonance region. The height of the barrier here proved to be $E_f^{1/2+} = 6.328$ MeV, taking the curvature as $\hbar\omega = 0.8$ MeV, as follows from systematics.

The fission barrier parameters for the other states were so chosen as to describe the experimental values appearing in Refs. [23, 24] and making a smooth link with the fission cross-section from the fast region. For this purpose it is necessary to introduce the following increases over the fission threshold of state $1/2^+$:

The evaluated mean fission widths are given in Table 2.8.

The energy dependence of the mean radiation widths $\langle\Gamma_\gamma\rangle(E)$ were determined by the gamma cascade emission model (section 4.3). Since the dependence of $\langle\Gamma_\gamma\rangle$, predicted by this model, on channel spin (in the absence of dependence of level density on parity) is considerably less than the experimental error $\Delta \langle\Gamma_\gamma\rangle \sim 1\%$, as determined in the resolved resonance region $\langle\Gamma_\gamma\rangle$ is taken as independent of state spin (Table 2.9).

The number of degrees of freedom of mean width distribution required for calculation of the mean cross-sections was determined by the number of open channels contributing to the average width (Table 2.10).

2.3. Analysis of results obtained

The lack of experimental data for σ_t, σ_n and σ_{nn} in the unresolved resonance energy region makes it impossible to carry out a comparison of experimental and evaluated cross-sections. Comparison is possible only between the radiative capture cross-sections (Fig. 2.1). Calculations for the mean resonance parameters were carried out as far as the excitation threshold of level 6^+ (approx. 300 keV) taking account of the competition from inelastic scattering at level 4^+. The strength functions for this state were calculated by the coupled-channel method: $S_o^{4+} = 0.78 \times 10^{-4} (\text{eV})^{-1/2}$, $S_1^{4+} = 3.0 \times 10^{-4} (\text{eV})^{-1/2}$.

It will be seen from the figure that the evaluated $\sigma_{n\gamma}$ figures are in good agreement with the experimental data of Ref. [72]. In the region up to ~ 10 keV our evaluation virtually coincides with the data of Refs [19, 72]. From 10 to 50 keV it lies between the results of the studies reported in Refs [19] and [20], which coincide within the limits of error. Between 50 and 160 keV the evaluation is somewhat lower than the data contained in Ref. [20], practically within the limits of experimental error, and further coincides with the results of studies [21-22]. As the calculations showed, it is impossible to describe the experimental data with a single parameter for the entire 1-300 keV region, unless account is taken of the difference in the values of the strength functions for the ground and excited states.

It will be seen from Fig. 2.2 that the calculated value for $\sigma_{n\gamma}(E)$ with the same strength functions for the ground and for the excited states lies lower than the experimental data within the area above the threshold for the (n,n') reaction. Since comparison in terms of σ_t is impossible owing to the absence of experimental data, the potential scattering cross-section σ_p is taken as $11.4 \times 10^{-28} m^2$, starting from calculations with a generalized optical model and evaluation in the resolved resonance region. The cross-section values for energies in the range 1-150 keV, calculated from evaluated mean parameters, are quoted in Table 2.11. The inelastic scattering cross-section $\sigma_{nn'}$ was calculated taking account of the contribution by the direct process mechanism.

3. ^{236}U FISSION CROSS-SECTION IN THE FAST NEUTRON ENERGY RANGE

Fission cross-section measurements for ^{236}U can be divided into two main groups. The first group comprises measurements of $\sigma_f(^{236}U)$ relative to the cross-sections for ^{235}U, while the second group contains a number of direct measurements. Methods of measuring the cross-section ratios do not require determination of the neutron flux, and hence the value of the data derived from the relationships increases in proportion to the degree of refinement of the reference cross-sections.

3.1. Experimental data on fission cross-sections in the 0.15-20 MeV energy range

The following experimental data regarding the ratio $\sigma_f(^{236}U)/\sigma_f(^{235}U)$ are available:

1. White, et al., [23] carried out measurments at three energy points (127, 312 and 505 keV) with errors of ~ 50, 40 and 10%.

2. White and Warner [29] determined the ratio at energies 1.0, 2.25, 5.4 and 14.1 MeV with errors of not more than 3%.

3. Lamphere and Greene [30] carried out measurments in the 0.7-4 MeV range with errors decreasing from ~ 20 to 2.5% with increasing energy.

4. Stein, et al., [31] determined the ratio of cross-sections for energies 1-5 MeV with errors of 2% for an energy in the region of 1 MeV and 1% in the remaining range.

5. Behrens and Carlson [32] measured the ratios in a wide energy range from 0.17 to 33 MeV with errors ~ 4% up to 0.6 MeV, ~ 2% from 0.6 to 0.9 MeV, ~ 1.5% from 0.9 to 2.3 MeV, ~ 2% from 2.3 to 10 MeV, and errors further rose to ~ 4% with increasing energy.

6. Nordborg, et al., [33] determined the ratio in the energy range 3.2-8.6 MeV with errors which increased as a function of energy from 1.5 to 2.5%.

7. Meadows [34] carried out measurements at energies 0.6-10 MeV with errors of 1-2%.

8. Goverdovskij, et al., [35] determined the ratio in the energy range 4-10.5 MeV with errors of 1-1.5%.

9. Fursov, et al., [36] measured the ratio in the energy range 0.34-7.4 MeV with errors of 1.5-2%.

10. The ratio of the fission cross-sections for ^{236}U to the fission cross-section for ^{238}U [37] and ^{235}U were also measured in an old study [38]: $\sigma_f(^{236}U)/\sigma_f(^{238}U) = (1.593 \pm 0.97)\%$ for $E_n = 14.5$ MeV; $\sigma_f(^{236}U)/\sigma_f(^{235}U) = (0.697 \pm 2)\%$ at 2.5 MeV and $(0.783 \pm 2.2)\%$ at 14.1 MeV.

Apart from the measurements of ratios there is an absolute measurement of the ^{236}U fission cross-section at energies of 2.6 and 14.7 MeV [39]: $(0.89 \pm 0.04) \times 10^{-28} m^2$ and $(1.62 \pm 0.08) \times 10^{-28} m^2$ respectively.

3.2. Evaluation of the fission cross-section for ^{236}U and the ratio $\sigma_f(^{236}U)/\sigma_f(^{235}U)$

From the available experimental data on $\sigma_f(^{236}U)$ and with the help of the presently-adopted standard fission cross-section for ^{235}U [40], we have derived absolute values for $\sigma_f(^{236}U)$ (Figs 3.1-3.5).

It will be seen from the figures that the data in the most accurate studies [32, 34-36], with the exception of certain points, coincide within the limits of experimental error. The data in Ref. [30] for energies above 3 MeV lie systematically 5-10% higher, while the results in Ref. [31] are, throughout practically the whole measured range, lower than the data from other experiments by 7-10%. The results in Ref. [33] at energies of 2-5 MeV and 7-9 MeV are located lower than the main group of data. In the region of the threshold for the $(n,n'f^{o})$ reaction at 6-7 MeV, the data in Ref. [32] are lower than the others, although remaining within the limits of error and not contradicting them.

The evaluated curve was drawn taking account of errors in the experimental data, but disregarding errors in $\sigma_f(^{235}U)$, and in the range 0.15-3 MeV is governed by the data in Refs [30, 32, 34, 36], in the range 3-7 MeV by the results of Refs [32, 34-36], in the range 7-10 MeV by the data from Refs [32, 34, 35] and thereafter follows Ref. [32], taking account of the results of the absolute measurement at 14.7 MeV in Ref. [39]. The energy dependence of σ_f above 10 MeV has been measured in a single study [32], and not sufficiently reliably. It was refined using calculations of partial cross-sections (n,2nf) and (n,3nf) on the basis of a statistical model (cf. section 5).

The errors reported by the authors of the experimental studies are small, and hence have been evaluated by us on the basis of the actual spread of the experimental data (Table 3.1).

Table 3.2 gives the evaluated data for the ratio $\sigma_f(^{236}U)/\sigma_f(^{235}U)$ in the energy range 0.15-20 MeV. In Figs 3.1-3.5 the present evaluation is compared with the ENDF/B-V evaluation [63]. It will be seen that the results of the present evaluation are somewhat lower (on average by 3-7%) than the ENDF/B-V data.

4. CROSS-SECTIONS FOR THE INTERACTION OF NEUTRONS WITH THE ^{236}U NUCLEUS IN THE FAST NEUTRON ENERGY RANGE 0.15-20 MeV

Experimental data on the cross-sections for the interaction of neutrons with the ^{236}U nucleus in the energy range 0.15-20 MeV, apart from σ_f and $\sigma_{n\gamma}$ up to 4 MeV, are not available. Hence, evaluation of the neutron data for these energies has been carried out on the basis of calculations with generalized optical and statistical models.

4.1. Optical cross-sections

Recently, extensive use has been made of the coupled-channel method [41] for evaluating and predicting the neutron cross-sections for heavy deformed nuclei. Given correct choice of the potential parameters it is possible with this method to describe all the experimental data for optical cross-sections [42, 43], and in the absence of information to predict the total cross-section, the compound nucleus formation cross-section, the direct elastic and inelastic neutron scattering cross-sections, their angular distributions, and also the generalized coefficients of transparence thereafter used in calculations under the statistical model. In Ref.[44] we derived generalized optical model potential parameters unique for the actinide group. The use of potential [44] for the specific nucleus requires only definition of its β_2 and β_4 deformation parameters. Available microscopic calculations of the deformation parameters [45, 46] do not yield a unique determination of their values, but predict with sufficient reliability their order of magnitude and isotopic dependence. Use of this dependence and of the β_2 and β_4 values for ^{238}U selected by us in Ref.[44] made it possible to derive β_2 and β_4 for the ^{236}U nucleus. The value of β_2 was then refined by fitting the strength function S_o calculated from the optical model to its value evaluated from the resolved resonance region. This fully defined the parameters of the optical potential:

$$V_R = 45{,}97-0{,}3E,\ \mathrm{MeV};\quad r_R = 1{,}256\ f;\quad a_R = 0{,}626\ f;$$

$$W_D = \begin{cases} 3{,}02+0{,}4E & (E \leq 10\ \mathrm{MeV})\ ; \\ 7{,}02 & (E > 10\ \mathrm{MeV})\ ; \end{cases}\qquad r_R = 1{,}260\ f;\quad a_D = 0{,}555\pm0{,}0045E\ f;$$

$$W_{so} = 7{,}5\ \mathrm{MeV};\quad \beta_2 = 0{,}213;\quad \beta_4 = 0{,}090.$$

These parameters were used for determining the optical cross-sections for ^{236}U by the coupled-channel method. The calculated values of the strength functions and the potential scattering cross-section were: $S_o = 1.164 \times 10^{-4} (eV)^{-1/2}$, $S_1 = 1.74 \times 10^{-4} (eV)^{-1/2}$, $\sigma_p = 11.42 \times 10^{-28} m^2$. Up to energies of about 5 MeV the calculations were effected taking account of the linkage of the first three levels of the basic rotational band, and at higher energies in an adiabatic approximation owing to the need to allow for excitation of a larger number of levels.

Figures 4.1-4.3 show the evaluated values of the excitation cross-sections for the first two levels and the cross-sections for compound nucleus formation. In Figs 4.1-4.2 the results of the present study are compared with the ENDF/B-V evaluation [63] regarding the excitation functions of the levels at 45.24 and 149.48 keV. It will be seen that in the evaluation performed in Ref.[63] no account was taken of the direct excitation process of these levels and therefore the inelastic scattering cross-section for these levels is equal to zero at an incident neutron energy of ~ 2 MeV. It should be pointed out that the potential parameters [44] were derived for incident neutron energies of up to 15 MeV and to some extent overestimated the experimental data for σ_t in the narrow energy range 15-20 MeV. Hence the calculated values for $\sigma_t(^{236}U)$ have been slightly corrected (within limits of 2-3%) allowing for the relationship between the calculated and experimental values of the total cross-section for ^{238}U. The maximum divergence between the evaluated and the calculated values for σ_t was 3% at 20 MeV.

4.2. Calculations using a statistical model

The cross-sections for processes passing through the compound nuclear stage were calculated with a statistical model for nuclear reactions. The effectiveness of this model, an analysis of calculational results and a comparison of theoretical and experimental data are described or given in Ref.[43]. The present study employs the results of the above analysis. In the calculations use is made of the following ^{236}U nucleus level scheme [47], given in Table 4.1.

At higher energies there is substantial omission of levels, hence the experimental information on the level scheme was not used and the density was regarded as a continuous dependence. Consequently, in the region of energies for excitation of the discrete level spectrum the calculations were carried out with the Hauser-Feshbach-Moldauer formalism [48, 49], taking account of corrections for partial width fluctuations, and at higher energies were performed in accordance with the formalism of Tepel, et al., [50].

The continuous level density required for the calculations was determined from the superfluid model of the nucleus taking account of vibrational and rotational modes [25, 26]. The model parameters were taken from Ref.[51].

Radiative capture transmissions were calculated by the gamma cascade emission model, with allowance for competition by fission and emission of neutrons in the successive cascades of the γ-discharge [52]. The energy dependence of the spectral factor $f(E,\varepsilon_\gamma)$ was regarded as a two-humped

Lorentz dependence, following from the photo-absorption cross-section [53], with parameters derived from heavy nucleus systematics [54]. The normalization of $f(E,\varepsilon_\gamma)$ was determined by the value $<\Gamma_\gamma>-(E=0) = 22.77$ meV. The fission transmissions were calculated allowing for the two-humped structure of the fission barrier and for collective, superfluid and shell effects in the fission channel level density [55]. Calculations by a statistical model underlay the evaluation of the radiative capture cross-section and the compound part of the elastic and inelastic scattering cross-sections. The neutron transmission coefficients, required for calculating by the statistical model, were determined by the coupled-channel method. Since this way of calculating radiative capture cross-sections does not take account of the possibility of direct and semi-direct capture, the cross-section $\sigma_{n\gamma}$ in the energy range above 5 MeV was made to satisfy, in the 10-20 MeV range, the value ~ $1.10^{-31}m^2$ predicted by systematics. Figure 4.4 compares the evaluated and experimental data for the radiative capture cross-section. The evaluation is in good agreement with the results given in Refs [21, 22] and [56]. The data in Refs [57, 58] lie appreciably higher than those from other experiments and it is not possible to describe them assuming any reasonable values of the model parameters. Comparison with the results of the ENDF/B-V evaluation [63] (Fig. 4.4) shows that the evaluation [63] is systematically higher (by ~ 40%) than the data in the present study. This difference in evaluations is reflected in the available experimental data. The results of our evaluation are confirmed by the latest experiments [21, 22, 56].

Figure 4.5 compares the total cross-sections and the elastic and inelastic scattering cross-sections obtained in the present investigation and in Ref. [63]. In terms of the total cross-section in the 0.1-1.0 MeV range, the ENDF/B-V evaluation [63] is higher than the results of the present evaluation by ~ 10%, while in the range 2-20 MeV both evaluations agree to within 3%. When comparing the results of the two σ_n and $\sigma_{nn'}$ evaluations for ^{236}U the same tendency as in the case of ^{235}U is observed: the elastic scattering cross-section in the ENDF/B-V evaluation is greater than the results of the present work in the 1-2 MeV range by 20%, while the inelastic scattering cross-section is ~ 20% less. As in the case of ^{235}U, in the 1-2 MeV range this may be explained by the fact that in evaluation [63] the contribution from low-lying levels, on which inelastic scattering of neutrons occurs, is included in the elastic channel. The higher values for ^{236}U obtained in the present work for the range 1-5 MeV are the result of taking account of the contribution by direct processes at the low-lying levels. At higher energies the greater $\sigma_{nn'}$ cross-section values reflect allowance for pre-equilibrium effects, which was done in the present work.

The evaluated figures for the σ_t, σ_n, $\sigma_{n\gamma}$, $\sigma_{nn'}$, σ_f, σ_{n2n} and σ_{n3n} cross-sections in the energy range 0.16–20.0 MeV are given in Table 4.2. The evaluated cross-sections for excitation of discrete levels and continuous spectrum are given in Table 4.3.

5. EVALUATION OF CROSS-SECTIONS FOR THE (n,xn) AND (n,xnf) REACTIONS

In view of the lack of experimental data on the cross-sections for the (n,2n) and (n,3n) reactions, the results of existing evaluations show substantial discrepancies. This is associated with divergences in the evaluation both of neutron-optical cross-sections and of emission fission contributions, calculation of which is based on extrapolation of the energy dependence of the fission cross-section from the first "plateau" region into the high excitation region. Thanks to the availability of a large volume of experimental data, the neighbouring isotope ^{238}U constitutes a unique opportunity for a coherent analysis of experimental data for the (n,2n), (n,3n) and (n,f) reaction cross-sections and for the secondary neutron spectra. The results of an analysis of this kind [59] formed the basis for the evaluation of the (n,2n) and (n,3n) cross-section reaction for ^{236}U.

5.1. Statistical description of the cross-sections for the (n,2n), (n,3n) and (n,f) reactions

For describing the fission and neutron cascade emission cross-sections use was made of a statistical model providing for conservation of spin and parity at all cascades in the decay of the ^{237}U compound nucleus [60]. The neutron transparences were calculated on the basis of a generalized optical model with potential parameters as described in section 4.2. In the energy range concerned, fission may be regarded as a two-stage process of successive passage through a two-humped barrier. A detailed description of this model and its application to the analysis of the fission cross-sections for U and Pu isotopes in the first "plateau" region is given in Ref. [55]. Here we shall mention only the principal features. For calculating the level density in the transient states and the neutron channel use was made of a phenomenological model [26], taking coherent account of shell, superfluid and collective effects. In this approach, the shell effects are modelled by the energy dependence of the level density parameter:

$$a(U) = \begin{cases} \tilde{a}\left[1 + \delta W \dfrac{f(U - E\quad)}{U - E}\right], & U \geq U \quad , \\ a(U\quad) & U < U \quad , \end{cases}$$

where a is the asymptotic value of the level density parameter at high excitation energies; δW is the shell correction to nuclei deformation energies; $f(U) = 1 - \exp(\lambda U)$ is a dimensionless function defining the change in the shell effects; and U_{cr} and E_{cond} are the critical energy of phase transfer and condensation energy. The collective effects are covered in accordance with the generalized model concept:

$$\rho(U,J^{\pi}) = \rho_{cr}(U,J^{\pi})\, K_{vib}(U)\, K_{rot}(U) \quad ,$$

where ρ_{cr} is the density of quasi-partial excitations of the nucleus, and K_{rot} are the coefficients of increase in level density through vibrational and rotational excitations. Shell corrections under conditions of equilibrium deformation are calculated according to the liquid-drop model. The correlation functions Δ_o are selected on the basis of the even-odd differences in nuclear binding energy. The shell corrections in the fissioning channel $\delta W_f^A = 2.5$ MeV and $\delta W_f^B = 0.6$ MeV are taken from Ref. [61]. The correlation functions Δ_f are selected from the description of the energy dependence of σ_f in the first "plateau" region on the assumption of complete asymmetry of the fissioning nucleus configuration in the region of the first hump and of mirror asymmetry in the region of the second. Mirror asymmetry leads to a doubling of level density, while axial asymmetry in an an increase in level density by $\sqrt{2\pi}\sigma_{||}$ times ($\sigma_{||} = \sqrt{F_{||}}t$, $F_{||}$ is the parallel moment of inertia of the fissioning nucleus, and t is the thermodynamic temperature). For description of the cross-sections (n,nf) and (n,xn) for reactions near the thresholds, the level density in the neutron channel is conceived in terms of a constant temperature model [51]:

$$\rho(U,J^{\pi}) = \frac{1}{\bar{T}_n} \exp\left(\frac{U-E_o}{\bar{T}_n}\right) \frac{2J+1}{2\sigma^2_{exp}} \exp\left(-\frac{J(J+1)}{2\sigma^2_{exp}}\right) \quad ,$$

where $\bar{T}_n = 0.385$ MeV; $\sigma^2_{exp} = 0.156\ A - 26.76$.

The point of linkage of the models $U_c = 10.72 - n\cdot\Delta_o - 0.028\ A$, $E_o \sim -n\Delta_o$, $n = 1, 2, 3$ for even-even, odd-even (even-odd) and odd-odd nuclei respectively. The spin dependence parameter for σ^2 is σ^2_{exp} up to excitation energies $U_{rp} = 1.2$; 0.6; 0.3 MeV for even-even, odd-even (even-odd) and odd-odd nuclei. Above this, up to energy U_c, σ^2 values were determined by linear interpolation between σ^2_{exp} and $\sigma^2_{\perp}(U_c) = F_{\perp}\cdot t$.

The dependence of the level density asymptotic parameter a on mass number A here has the form

$$\tilde{a} = 0.484\ A - 0.0016\ A^2$$

The density of the lower transient fission states was described in the same manner. The temperature T_f was determined from the condition:

$$\frac{1}{T_f} e^{\frac{U_c - E_0}{T_f}} = \sigma_{\perp f}^2 \frac{\omega(U_{cf})}{\sqrt{2\pi}\,\sigma_{\parallel f}} \quad ;$$

$$U_{cf} = U_c ; \sigma_{\perp f}^2 = \sigma_{\perp f}^2 (U_{rp}) \quad \text{for} \quad U < U_{rp} \quad ;$$

$$\sigma_{\parallel f}^2 = \sigma_{\parallel f}^2 (U_{rp}) \quad \text{for} \quad U < U_{rp} \quad ;$$

$$E_0 = -n\Delta_f \; ; \quad \tilde{a}_f = \tilde{a}_n \quad ,$$

where $\omega(U_{cf})$ is the inner excitation density; $T_f = T_n = 0.385$ MeV; $\Delta_f = \Delta_o + 0.08$ MeV. Such an approximation $U_{cf} = U_c$ for the level density makes it possible to describe σ_{nf} and σ_{n2n} near the thresholds. To describe the cross-sections for the (n,f), (n,2n) and (n,3n) reactions throughout the energy range recourse was had to parameterization of the hard portion of the inelastically scattered neutron spectrum in the excitation model [62]. Here the principal parameter, the matrix element of the double-quasi-partial interactions M^2, was taken as equal to $10/A^3$, as for ^{238}U. The fission barriers for the ^{237}U, ^{236}U, ^{235}U and ^{234}U compound nuclei, derived from the description of the fission cross-sections in the first "plateau" region, are given in Table 5.1, and the level density and transient state parameters for fission of uranium isotopes are given in Table 5.2. The fission cross-sections as calculated on the basis of the model described above differ from the experimental data in the 2-20 MeV range by not more than 3-4% (Fig. 5.1). The "first chance" fission cross-section shown in this figure is not constant, but decreases by ~ 30% when the energy is increased to 20 MeV. The cross-sections $\sigma_{n,2n}$ and $\sigma_{n,3n}$ (Fig. 5.2), renormalized to take account of the slight differences in the calculated and evaluated fission cross-sections, are given in Table 4.1.

6. ENERGY AND ANGULAR DISTRIBUTIONS OF SECONDARY NEUTRONS AND THE QUANTITY $\bar{\nu}_p(^{236}U)$

Experimental data on neutron energy and angular distributions are completely lacking. Hence, evaluation was based on theoretical calculations. In section 5, we described the model which in principle made it possible to derive not only the cross-sections for the neutron successive emission reactions but also their energy distributions. Unfortunately, available computer programs [60] permit calculations only of the sum spectra for the (n,n'x), (n,2n'x) etc. reactions with no definition of the subsequent source (x) of the decay of the nucleus.

6.1. Evaluation of secondary neutron energy spectra

For calculating the energy distributions of secondary neutrons use was made of a simple model, disregarding the dependence on spin J, but making it possible to derive the neutron spectra for specific (n,n'γ), (n,2n) and (n,3n) reactions.

In accordance with what was stated in section 5, it was assumed that a part of the neutrons can be emitted from the nucleus before static equilibrium is established in it (pre-equilibrium neutrons). The equilibrium part of the first neutron spectrum was modelled on Ref. [65].

$$I_p^1(E_n, E') = E'\sigma_c(E_n, E')\rho(E_n - B_n - E') ,$$

where E_n is incident neutron energy; E' is the energy of the emitted neutron; $\sigma_c(E_n,E')$ is the cross-section for the reaction inverse to neutron emission; ρ is the density of the residual state of the nucleus; and B_n is the separation energy of the neutron.

The sum spectrum of the first neutron is the sum of the pre-equilibrium and equilibrium spectra with the fractions as determined in section 5. This spectrum governs the distribution of residual nuclei excitation after emission of the first neutron $\chi'(E)$. It is then easy to derive the distribution of the probability of nuclear excitations after the escape of the (n+1)-th neutron:

$$\chi^{n+1}(E) = \int_{E+B_n}^{E_n} \chi^n(E') S(E', E)\, dE' ,$$

where S(E',E) is the probability of nucleus A with excitation E' emitting a neutron with energy $E'-E-B_n$ and becoming nucleus A-1 with excitation E.

The probability S(E',E) is normalized by the condition:

$$\int_0^{E'-B_n} S(E',E)\,dE = \Gamma_n(E')/\Gamma(E') ,$$

where $\Gamma_n(E')$, $\Gamma(E')$ are the neutron and total widths.

Considering that the second and subsequent neutrons are emitted from the equilibrium state, spectrum $I_p^{(1)}$ governs S(E',E) with an accuracy up to the normalization f(E'):

$$S(E',E) = f(E')\sigma_c(E'-B_n-E)\cdot(E'-B_n-E)\rho(E)\ ,$$

where

$$f(E') = \frac{\Gamma_n(E')}{\Gamma(E')\int_0^{E'-B_n}\sigma_c(E'-B_n-E)(E'-B_n-E)\rho(E)dE}$$

bearing in mind that $\sigma_c(E,E') = \sigma_c(E')$.

The spectrum for the second neutron of the (n,2n) reaction was determined by the formula

$$I^{(2)}(E_n,E') = \int_{B_{nA}+E}^{E_n} x'(\varepsilon)\, S(\varepsilon,\varepsilon-B_{nA}-E')d\varepsilon\ .$$

The spectrum for the third neutron of the (n,3n'x) reaction:

$$I^{(3)}(E_n,E') = \int_{B_{nA-1}+E'}^{E_n-B_{nA}} x^2(\varepsilon)\, S(\varepsilon,\varepsilon-B_{nA-1}-E')d\varepsilon\ .$$

The spectrum for neutrons of the (n,n'γ) reaction

$$I_{nr'}(E_n,E') = I^{(1)}(E_n,E')\,\frac{\Gamma_{\gamma A}(E_n-E')}{\Gamma_A(E_n-E')}\ .$$

The spectrum for the first neutron of the (n,2n) reaction

$$I^{1}_{n,2n}(E_n,E') = I^{1}(E_n,E')\cdot P_1(E_n,E_n-E')\ ,$$

where

$$P_1(E_n,E_n-E') = \begin{cases} 0\ , & \text{if } E'>E_n-B_{nA} \\ \int_0^{E_n-E'-B_{nA}} S(E_n-E',\varepsilon)\frac{\Gamma_{\gamma A-1}(\varepsilon)}{\Gamma_{A-1}(\varepsilon)}d\varepsilon, & \text{if } E'<E_n-B_{nA}, \end{cases}$$

and for the second neutron of the (n,2n) reaction

$$I^{2}_{n,2n}(E_n,E') = \int_{E'+B_{nA}}^{E} x'(\varepsilon)\, S(\varepsilon,\varepsilon-B_{nA}-E')\frac{\Gamma_{\gamma A-1}(\varepsilon-B_{nA}-E')}{\Gamma_{A-1}(\varepsilon-B_{nA}-E')}d\varepsilon\ .$$

Similar expressions can be written for the spectra of the successively emitted neutrons in the (n,3n), (n,n'f), (n,2n'f) reactions and so on. As will be seen from the formulae quoted above, the secondary neutron spectrum integrals govern the cross-sections for the corresponding reactions. When evaluating the spectra, the level density necessary for the calculation was taken from the Fermi-gas model [66]. The basic parameter of the model, the level density a, was selected in such a way that the calculations for the spectra of the (n,n'x), (n,2n'x) and (n,3n'x) reactions coincided with the calculation of these quantities on the basis of a point model (see section 5). It turned out that with the same pre-equilibrium process contributions agreement is reached at a value of $a = 30\ MeV^{-1}$. In addition, the calculated values of the cross-sections for the (n,2n), (n,3n) reactions are in good agreement if use is made of the relation Γ_f/Γ_n, in the fast energy region, fitted to the experimental values [67]. As an example, Fig. 6.1 shows the secondary neutron spectra for an incident neutron energy of 14 MeV.

6.2. Evaluation of secondary neutron angular distributions

The angular distributions of neutrons from reactions proceeding through the compound nuclear stage were taken to be isotropic. Anisotropy is considered only for elastic scattering and inelastic scattering on the first two excited levels. The coefficients of expansion into Legendre polynomials of the angular distributions of neutrons at these levels were calculated from a generalized optical model with allowance for the compound contribution.

Figures 6.2 and 6.3 show the angular distributions of elastically and inelastically scattered neutrons at energies of 4 and 14 MeV.

Owing to their voluminous nature, the coefficients of expansion of the angular distributions into Legendre polynomials and the secondary neutron energy spectra are not included in the text. They can be obtained from the complete file of evaluated nuclear data for ^{236}U, transmitted to the Nuclear Data Centre.

6.3. Fission neutron spectrum

Measurements of the spectra of neutrons emitted upon ^{236}U fission are not available. Hence the only source of information remains the application of systematics for the nuclei studied. The fission neutron energy spectrum is in the present study treated as a Maxwellian distribution:

$$N_M(E) = \frac{2}{(\pi T^3)^{1/2}} E^{1/2} \exp(-E/T).$$

In Ref. [68] it was shown that, although there are more complex expressions for fission neutron spectra, they all differ by < 4% in the energy range 0.01–6 MeV, and only as from ~ 10 MeV, when the neutron yield drops by more than two orders, do the differences reach 25%, which remains within the limits of measurement accuracy. In Ref. [68] it was determined that the mean fission neutron spectrum energy $\bar{E} = \frac{3}{2} T$ is in a first approximation a linear function of Z^2/A. Taking account of this relationship from the experimental data $\bar{E}(^{235}U + n_T) = 1.970 \pm 0.015$, $\bar{E} = (^{239}Pu + n_T) = 2.087 \pm 0.015$,

$\bar{E}(^{233}U + n_T) = 2.015 \pm 0.015$ [68] the mean energy of the spectrum of ^{236}U fission by thermal neutrons is:

$$\bar{E} = (^{236}U + n_T) = 1.948 \text{ MeV}.$$

It follows from systematics that the dependence of E on incident neutron energy has the form [69].

$$\bar{E} = a + b\,[1 + \nu_t\,(E)]^{1/2}.$$

The coefficients a and b in the second expression were so selected as to satisfy the value of $\bar{E}$ for the thermal point and to describe the growth in $\bar{E}$ by 1% (analogously with ^{235}U) [68], accompanied by an increase in excitation energy of 1 MeV: a = 0.799, b = 0.628.

6.4. The evaluated quantity $\bar{\nu}_t$ (E) ^{236}U

The quantity $\bar{\nu}_p$ was not evaluated. By way of evaluated figures for $\bar{\nu}_p$ data were taken from Ref. [70], in which, for energies below 6 MeV the evaluation was based on experimental data, while above 6 MeV it was based on systematics.

Measurements on neighbouring nuclei show that $\bar{\nu}_d(E)$ undergoes practically no change up to ~ 4 MeV, and then linearly decreases by ~ 40% up to an energy of ~ 8 MeV, after which it again does not change [71]. The value of $\bar{\nu}_d$ was selected having regard to the systematics of the behaviour of the experimental data for the uranium isotopes ^{233}U, ^{235}U and ^{238}U. Table 6.1 gives the evaluated figures for $\bar{\nu}_t$ and $\bar{\nu}_p$. As a standard, use was made of the quantity $\bar{\nu}_p(^{252}C_f) = 3.757 \pm 0.005$.

CONCLUSION

There are insufficient experimental data for the ^{236}U nucleus, and hence the reliability of evaluated data is governed to a large extent by the correctness of the theoretical models employed. In carrying out the present evaluation we have applied theoretical models which had been tested by reference to the available experimental data for ^{237}U, ^{235}U and ^{239}Pu. For purposes of analysis use was made of modern concepts, which permitted a more accurate determination of the excitation functions for the (n,n'), (n',2n) and (n,3n) reactions, and of the angular distributions of elastically and inelastically scattered neutrons, experimental data for which are completely lacking.

The evaluated data obtained for total cross section and elastic scattering cross-section are based on theoretical calculations using the coupled-channel method. The fission cross sections were evaluated on the basis of all the available experimental results. The evaluation of the radiative capture cross-section which we carried out confirms the latest experimental data obtained in the USSR, which lie ~ 40% below the results previously obtained.

Resonance parameters were obtained, describing all available experimental data in the thermal and resonance energy ranges. For unresolved resonance energies, a theoretical prediction is made for the cross sections σ_t, σ_n and $\sigma_{nn'}$, for which experimental data are lacking. Still open remains the question of the degree of reliability of introducing corrections for level omission, since the available methods give values of <D> diverging by ~ 10%.

The complete system, established in the present study, of evaluated nuclear data for ^{236}U in the energy range from 10^{-5} eV to 20 MeV was recorded on magnetic tape in ENDF/B format and transmitted to the Nuclear Data Centre of the State Committee on Atomic Energy. The system has been created with the use of correct theoretical models, reflecting contemporary physical concepts, and taking account of the total available experimental results. A comparison of these data with the ENDF/B-V evaluation shows the inadequacy of the latter evaluation in the light of contemporary concepts.

REFERENCES

[1] SINEV, N.M., BATUROV, B.B., Principles of the technology and economics of nuclear fuel, Atomizdat, Moscow (1980) 342.

[2] SANTAMARINA, A., DARROUZET, M., MARTIN DEIDIER, L., Nuclear data qualification through French LWR integral experiment. Proc. Conf. on Nuclear Data for Basic and Applied Science (May 1985) Santa Fe, USA.

[3] KUESTERS, H., Testing of evaluated transactinium isotope neutron data and remaining data requirements. Proc. of the Advisory Group Meeting on Transactinium Isotope Nuclear Data, Uppsala, 1984. Vienna: IAEA (1985) 9-55.

[4] KRAVTSOV, V.A., Atomic masses and nuclear binding energies, Atomizdat, Moscow (1974) 344.

[5] HOWERTON, R.T., Thresholds of nuclear reactions induced by neutrons, photons, deutrons, tritons and alpha particles. UCRL-50400, TID-4500, UC-34 (1970) Vol. 9, 304.

[6] BELEN'KIJ, A.N., SKOROKHVATOV, M.D., EhTENKO, A.V., Measurement of the characteristics of ^{238}U and ^{236}U spontaneous fission, At. Ehnerg. 55 2 (1983) 97.

[7] HARVEY, J.A., HUGHES, D.J., Spacing of nuclear energy levels. Phys. Rev. (1958) Vol. 109, 471-479.

[8] CARRARO, G., BRUSEGAN, A., Total neutron cross-section measurements of ^{236}U in the energy range 40 eV to 4.1 keV. Nucl. Phys. (1976) Vol. A257, 333-347.

[9] MEWISSEN, L., POORTMANS, F., ROHU, G. et al., Neutron cross-section measurements on ^{236}U. Nuclear cross-sections and Technology: Proc. of a Conf., Washington (1975) Vol. 2, 729-732.

[10] CARLSON, A.D., FRIESENHAHN, S.J., LOPEZ, W.M., FRICKE, M.P., The ^{236}U neutron capture cross section. Nucl. Phys. (1970) Vol. A141, 577-591.

[11] HARLAN, R.A., Total neutron cross-section parameters ^{236}U. INDC(US), 10 U, Vienna (1969) 60.

[12] McCALLUM, W., The neutron total cross sections of uranium-234 and uranium-236. Journ. of Nucl. Energy (1958) Vol. 6, 181-190.

[13] THEOBALD, J.P., WARTENA, J.A., WEIGMANN, H., POORTMANS, F., Fission components in ^{236}U neutron resonances. Nucl. Phys. (1972) Vol. A181, 639-644.

[14] BERRETH, J.R., SCHUMAN, R.P., Measurement of resonance integral. Reports to the AEC Nuclear Cross Sections Advisory Group. USAEC Report WASH-1041, Brookhaven, National Laboratory (1962) 37.

[15] CABELL, M.J., EASTWOOD, T.A., CAMPION, P.J., The thermal neutron capture cross section and resonance capture integral of ^{236}U. Journ. of Nucl. Energy (1958) Vol. 7, 81-87.

[16] HALPERIN, J., STOUGHTON, R.W., Some cross sections of heavy nuclides important to reactor operation. Proc. of Second Conf. on Peaceful Uses of Atom. En., Geneva (1958) Vol. 16, 64.

[17] YUROVA, L.N., POLYAKOV, A.A., RUKHLO, V.P. et al., Integral radiative capture cross sections in the thermal and resonance energy regions for ^{230}Th, $^{231-233}Pa$, ^{236}U and ^{237}Np, Vopr. atom. nauki i tekhniki, Ser. Yader. Konstanty 1 55 (1984) 3.

[18] PORODZINSKIJ, Yu.V., SUKHOVITSKIJ, E.Sh., Method for determining average neutron widths and average level spacings taking account of the final resolution of the experimental apparatus, Vestsi Akad. navuk BSSR, Ser. Fiz.-Ehnerg. Navuk 3 (1986).

[19] BERGMAN, D.A., MEDVEDEV, A.N., SAMSONOV, A.E. et al., Measurement of the neutron radiative capture cross-sections for ^{236}U in the 0.1-50 keV energy range. Vopr. atom. nauki i tekhniki, Ser. Yader. Konstanty 1 45 (1983) 3.

[20] KAZAKOV, L.E., KONONOV, V.N., POLETAEV, E.D. et al., Measurement of the neutron radiative capture cross-sections for ^{236}U and ^{197}Au in the 3-420 keV energy range. Vopr. atom. nauki i tekhniki, Ser. Yader. Konstanty 2 (1985) 44.

[21] GRUZDEVICH, O.T., DAVLETSHIN, A.N., TIPUNKOV, A.O. et al., Cross-section for radiative capture of neutrons by ^{236}U nuclei in the 0.15-1.1 MeV energy range. Vopr. atom. nauki i tekhniki, Ser. Yader. Konstanty 2 51 (1983) 3.

[22] DAVLETSHIN, A.N., TIPUNKOV, A.O., TIKHONOV, S.V., TOL'STIKOV, V.A., Cross-section for radiative capture of neutrons by ^{197}Au, ^{236}U, ^{237}Np nuclei. At. Ehnerg. 58 3 (1985) 183.

[23] WHITE, P.H., HODGKINSON, J.G., WALL, G.J., Measurements of fission cross-sections for neutrons of energies in the range 40-500 keV. Physics and Chemistry of Fission: Proc. of a Symposium, Salzburg, 1965. Vienna: IAEA (1965) Vol. 1, 219-233.

[24] PERKIN, J.L., WHITE, P.H., FIELDHOUSE, P. et al., The fission cross-sections of ^{233}U, ^{234}U, ^{235}U, ^{236}U, ^{237}Np, ^{239}Pu, ^{240}Pu and ^{241}Pu for 24 keV neutrons. Journ. of Nucl. Energy. Part A B (1965) Vol. 19, 423.

[25] BOR, A., MOTTELSON, B., The structure of the atomic nucleus, Mir, Moscow (1977) Vol. 2, 664.

[26] IGNATYUK, A.V., ISTEKOV, K.K., SMIRENKIN, G.N., The role of collective effects in the systematics of level density, Yad. Fiz. 29 (1979) 875.

[27] DRESNER, L., Inelastic scattering of neutrons by ^{238}U below 1 MeV. Nucl. Sci. Eng. (1961) Vol. 10, 142-150.

[28] KLEPATSKIJ, A.B., KON'SHIN, V.A., SUKHOVITSKIJ, E.Sh., The coupled-channel method and evaluation of the neutron data of fissioning nuclei, Vestsi Akad. Navuk BSSR, Ser. Fiz.-Ehnerg. Navuk 2 (1984) 21.

[29] WHITE, P.H., WARNER, G.P., The fission cross-sections of ^{233}U, ^{234}U, ^{236}U, ^{238}U, ^{237}Np, ^{239}Pu, ^{240}Pu and ^{241}Pu relative to that of ^{235}U for neutrons in the energy range 1-14 MeV. Journ. of Nucl. Energy (1967) Vol. 21, 671-679.

[30] LAMPHERE, R.W., GREENE, R.E., Neutron-induced fission cross-sections of ^{234}U and ^{236}U. Phys. Rev. (1955) Vol. 100, 763-770.

[31] STEIN, W.E., SMITH, R.K., SMITH, H.L., Relative fission cross-sections of ^{236}U, ^{233}U, ^{237}Np and ^{235}U. Neutron cross-sections and technology Proc. of a Conf., Washington (1968) 627-634.

[32] BEHRENS, J.W., CARLSON, G.W., Measurements of the neutron-induced fission cross-sections of ^{234}U, ^{236}U and ^{238}U relative to ^{235}U from 0.1-30 MeV. Nucl. Sci. and Eng. (1977) Vol. 63, 250-267.

[33] NORDBORG, C., CONDE, H., STROEMBERG, L.G., Fission cross-section ratio measurements of $^{232}Th/^{235}U$ and $^{236}U/^{235}U$. Neutron Physics and Nuclear Data: Proc. of an Intern. Conf., Harwell (1978) 910-915.

[34] MEADOWS, J.W., The fission cross-sections of uranium-234 and uranium-236 relative to uranium-235. Nucl. Sci. and Eng. (1978) Vol. 65, 171-180.

[35] GOVERDOVSKIJ, A.A., GORDYUSHIN, A.K., KUZ'MINOV, B.D. et al., Measurement of the ratios of the cross-sections for fission of ^{236}U and ^{235}U by 5.7-10.7 MeV neutrons. Neutron physics, TsNIIatominform, Moscow (1984) Vol. 2, 193.

[36] Measurement of the ratio of fission cross-sections for ^{236}U and ^{235}U in the neutron energy range 0.34-7.4 MeV. At. Ehnerg. 59 4 (1985) 284.

[37] NYER, W., Report LAMS-938 (1950).

[38] WAHL, J.S., DAVIS, R.W., Report LA-1681 (1954).

[39] FOMICHEV, A.V., Precision measurements of the cross-sections for fission of uranium, neptunium and plutonium isotope nuclei by fast neutrons, Dissertation for degree of Master of Physico-Mathematical Sciences, Leningrad (1984) 22.

[40] YANKOV, G.B., The ^{235}U fission cross-section. Nuclear Data Standards for Nuclear Measurements: Techn. Rep. Series N 227. Vienna: IAEA (1983) 39-45.

[41] TAMURA, T., Analysis of the scattering of nuclear particles by collective nuclei in terms of the coupled-channel calculation. Rev. Mod. Phys. (1965) Vol. 37, N 4, 679-708.

[42] LAGRANGE, Ch., Evaluation of nuclear-nucleons cross-sections in heavy nuclei with a coupled-channel model in the range of energy from 10 keV-20 MeV. Proc. of the EANDC Topical Discussion on Critique of Nuclear Models and their Validity in the Evaluation of Nuclear Data. Tokyo, JAERI-M-5984 (1975) 51-57.

[43] KON'SHIN, V.A., ANTSIPOV, G.V., SUKHOVITSKIJ, E.Sh. et al., Evaluated neutron constants for uranium-235. Nauka i tekhnika, Minsk (1985) 198.

[44] KLEPATSKIJ, A.B., KON'SHIN, V.A., SUKHOVITSKIJ, E.Sh., Optical potential for heavy nuclei, Vopr. atom. nauki i tekhniki, Ser. Yarder. Konstanty 1 45 (1982) 29.

[45] MOLLER, P., NILSSON, S.Q., NIX, J.R., Calculated ground-state properties of heavy nuclei. Nucl. Phys. (1974) Vol. A229, N. 2, 292-319.

[46] BEMIS, C.E., McGOWAN, F.K., FORD, T.L.C. et al., E2 and E4 transition moments and equilibrium deformation in the actinide nuclei. Phys. Rev. C. (1973) Vol. 8, N. 4, 1466-1480.

[47] SCHMORAK, M.R., Nuclear data sheets (1977) Vol. 20, 192.

[48] HAUSER, W., FESHBACH, H., The inelastic scattering of neutrons. Phys. Rev. (1952) Vol. 87, 366-386.

[49] MOLDAUER, P.A., Statistical theory of nuclear collision cross-sections. Phys. Rev. B. (1984) Vol. 135, N. 3, 642-659.

[50] HOFMANN, H.M., RICHER, T.J., TEPEL, J.W. et al., Direct reactions and Hauser-Feshbach theory. Annals of Physics (1975) Vol. 90, N. 2, 403-435.

[51] ANTSIPOV, G.V., KON'SHIN, V.A., MASLOV, V.M., Level density and radiation widths of transactinides, Vopr. atom. nauki i tekhniki, Ser. Yader. Konstanty, 3 (1985) 25.

[52] ZENEVICH, V.A., KLEPATSKIJ, A.B., KON'SHIN, V.A., SUKHOVITSKIJ, E.Sh., The possibility of predicting the radiative capture of neutrons by fissioning nuclei. Neutron Physics: Proc. of the 5th All-Union Conf. on neutron physics, Kiev, 1980, TsNIIatominform, Moscow (1980) Part 3, 245.

[53] NEYSSIERE, A., BEIL, H., BERGERE, R. et al., A study of the photofission and photoneutron processes in the giant dipole resonance of ^{232}Th, ^{239}U and ^{237}Np. Nucl. Phys. (1973) Vol. A199, N. 1, 45-64.

[54] LYNN, B.J.E., Systematics for neutron reactions of the actinide nuclei. Report AERE-R7469. Harwell (1974) 97.

[55] IGNATYUK, A.V., KLEPATSKIJ, A.B., MASLOV, V.M., SUKHOVITSKIJ, E.Sh., Analysis of the cross-sections for fission of U and Pu isotopes by neutrons in the first "plateau" region. Yad. Fiz. 42 3(9) (1985) 569.

[56] TOLSTIKOV, V.A., MANOKHIN, V.N., Status of neutron radiative capture data for ^{236}U and ^{237}Np. Proc. of the Third Advisory Group Meeting on Transactinium Isotope Nuclear Data, Uppsala, 1984. Vienna: IAEA (1985) 323-328.

[57] STUPEGIA, D.C., HENRICH, R.R., McCLOUD, G.H., Neutron capture cross-sections of ^{236}U. Journ. of Nucl. Energy, Part ASB (1961) Vol. 15, 200-203.

[58] BARRY, J.F., BUNCL, J.L., PERKIN, J.L., The radiative capture cross section of ^{236}U for neutrons in the energy range 0.3-4.0 MeV. Proc. Phys. Soc. (1961) Vol. 78, 801-807.

[59] GRUDZEVICH, O.T., IGNATYUK, A.V., MASLOV, V.M., PASHCHENKO, A.V., Consistent description of the cross-sections of the (n,nf) and (n,xn) reactions for transuranium nuclei. Neutron Physics, TsNIIatominform, Moscow (1984) Part 2, 318.

[60] UHL, M., STROHMAIER, B., Computer code for particle induced activation cross-sections and related topics. Report IRK-76-01. Vienna (1976) 30.

[61] ISTEKOV, K.K., KYPRIYANOV, V.M., FURSOV, B.I., SMIRENKIN, G.N., The applicability of traditional systematics to the probability of fission. Yad. Fiz. 29 5 (1979) 1156.

[62] SEIDEL, K., SEELIGER, D., REIF, P. et al., Pre-equilibrium decay in nuclear reactions. Physics of elementary particles and the atomic nucleus, 7 2 (1976) 499.

[63] DIVADEEMAN, M., MANN, F.M., McCROSSON, J. et al., ^{236}U Evaluated nuclear data file, Format B, Version V, US National Neutron Cross Section Centre, Brookhaven National Laboratory. Upton, New York (1979).

[64] HOWERTON, R.J., Livermore evaluated nuclear data library. MAT-7869. UCRL-5400 (1978) Vol. 15.

[65] BLATT, J., WEISKOPF, V., Theoretical nuclear physics, Moscow IL (1954) 659.

[66] MALYSHEV, A.V., Level density and structure of atomic nuclei, Atomizdat (Moscow) (1969) 144.

[67] SMIRENKIN, G.N., FURSOV, O.V., The dependence of heavy nuclei fission cross sections on neutron energy in the "plateau" region. Vopr. atom. nauki i tekhniki, Ser. Yader. Konstanty 2 (1988) 31.

[68] STAROSTOV, B.I., Prompt neutron spectrum for fission of ^{233}U, ^{235}U and ^{239}Pu by thermal neutrons and ^{252}Cf spontaneous fission spectrum in the 0.01-10 MeV energy range, Dissertation for degree of Master of Physico-Mathematical Sciences, Kiev (1984) 24.

[69] HOWERTON, R.J., DOYAS, R.J., Fission temperatures as a function of the average number of neutrons from fission. Nucl. Sci. Eng. (1971) Vol. 46, 414-416.

[70] MALINOVSKY, V.V., TARASKO, H.Z., KUZMINOV, B.D., Prompt neutron average number evaluation for neutron-induced fission. Proc. Conf. on Nuclear Data for Basic and Applied Science, May 1985. Santa Fe, USA (1985).

[71] MANERO, F., KON'SHIN, V.A., Status of the energy-dependent ν-values for the heavy isotopes (z > 90) from thermal to 15 MeV and of ν-values for spontaneous fission. Atomic Energy Review (1972) Vol. 10, N. 4, 637-756.

[72] MURADYAN, G.V., MURADYAN, Yu.V., VASKANYAN, M.A. et al., Measurement of capture cross-section and investigation of the spectrum of the multiplicity of neutron capture gamma quanta for ^{236}U: Report on NIR, I.V. Kurchatov Institute of Atomic Energy. Serial No. 50-05/113 Moscow (1985).

Table 1.1. Experimental and evaluated resonance parameter values.

Resonance No.	E_i, eV	Γ_{n_i}, MeV	Γ_γ, MeV	Γ_f,	Reference
I	2	3	4	5	6
0	- 4,54	8,406	2,0594	0,035	*
I	5,49 ± 0,049	I,76 ± 0,2I	-	-	/7/
	5,45	2,I6 ± 0,08	24,5 ± I		/I0/
	5,46	2,08 ± 0,I2	25,6		/II/
	5,45	I,95 ± 0,4	29 ± 7	0,29	/I3/
	5,49	2,I0	25,0	0,29	*
2	30,2 ± 0,I2	0,6I ± 0,II			/7/
	29,7	0,585 ± 0,03			/I0/
	29,8	0,568 ± 0,27			/II/
	29,9			0,I6	/I3/
	29,7	0,587	22,7	0,I6	*
3	34,6 ± 0,I2	2,6 ± I,2			/7/
	34,I2	2,4 ± 0,I2			/9/
	34,0	2,35 ± 0,I3	20,9 ± 3,5		/I0/
	34,I	2,22 ± 0,23			/II/
	34,0			0,I8	/I3/
	34,0	2,36	20,I4	0,I8	*
4	44,5 ± 0,I4	I9,0 ± 5			/7/
	43,92 ± 0,03	I7,5 ± 0,4			/8/
	43,90	I5 ± 0,7	I9,2 ± 2		/9/
	43,7	II,8 ± 0,6	22,0 ± I,5		/I0/
	43,9	II,33 ± I,I			/II/
	43,7			0,43	/I3/
	43,7	I4,09	I7,76	0,43	*
5	64,29	0,037 ± 0,005			/9/
	63,I	0,034 ± 0,005			/I0/
	63,I	0,037	22,77	0,354	*
6	72,3 ± 0,I8	40,0 ± I0,0			/7/
	7I,47 ± 0,06	24 ± 6			/8/
	7I,47	I8,5 ± 2	22, ± 2		/9/
	7I,I	I9,0 ± I,0	23,3 ± 0,9		/I0/
	7I,5	I7,76 ± I,8			/II/
	7I,I			0,29	/I3/
	7I,I	I8,73	23,36	0,29	*
7	87,4 ± 0,2	44,0 ± II			/7/
	86,5I ± 0,07	36 ± 9	20 ± I,6		/8/
	86,5I	28 ± I,5			/9/
	86,0	26,0 ± 2,0	24,3 ± I,3		/I0/
	86,4	28,8 ± 2,9			/II/
	86,4			0,30	/I3/
	86,0	28,56	2I,43	0,30	*
8	I02,25 ± 0,I4	0,75 ± 0,20			/8/
	I02,3	0,88 ± 0,04			/9/
	I0I,7	0,8 ± 0,08			/I0/
	I0I,7	0,88	22,77	0,354	*
9	I2I,0 ± 0,23	53,0 ± I9			/7/
	I20,95 ± 0,06	57 ± II			/8/
	I20,9	50 ± 2	20 ± I,5		/9/
	I20,2	5I,8 ± 4,0	24,0 ± I,5		/I0/
	I2I,0	57,2 ± 6,6			/II/
	I20,8			0,34	/I3/
	I20,2	50,8I	22,0I	0,34	*
I0	I26,0 ± 0,24	8,0 ± 4,0			/7/
	I24,88 ± 0,08	I7 ± 2			/8/
	I24,9	I7 ± 0,5	I9 ± 2,6		/9/
	I24,2	I5,9 ± I,9	2I,0 ± 3,5		/I0/
	I25,5	I3,44 ± 2,2			/II/
	I24,7			0,2I	/I3/
	I24,2	I6,7I	I9,62	0,2I	*
II	I33 ± 0,24	-			/7/
	I34,57 ± 0,II	I,4 ± 0,4			/8/
	I34,4	I,2 ± 0,04			/9/
	I33,7	I,08 ± 0,09			/I0/

Table 1.1. (cont.)

I	2	3	4	5	6
	I33,7	I,20	22,77	0,354	*
I2	I37,76	0,84 ± 0,30			/8/
	I37,8	0,57 ± 0,03			/9/
	I37,0	0,48 ± 0,I			/I0/
	I37,0	0,57	22,77	0,354	*
I3	I64,72 ± 0,I4	2,I ± 0,7			/8/
	I64,6	2,I ± 0,08			/9/
	I63,7	2,09 ± 0,I5			/I0/
	I63,7	2,I0	22,77	0,354	*
I4	I92,89 ± 0,I3	9,4 ± I,6			/8/
	I92,8	9,0 ± 0,3			/9/
	I92,6	I3,2 ± I,3			/I0/
	I92,6	9,0I	22,77	0,354	*
I5	I98 ± 0,30	94,0 ± 25,0			/7/
	I94,35 ± 0,I0	58 ± 6			/8/
	I94,3	44 ± I,3	20,0 ± I,5		/9/
	I94,0	52,0 ± I3,0	I8,0 ± 6,0		/I0/
	I94,0			0,50	/I3/
	I94,0	45,4I	I9,07	0,500	*
I6	2I6 ± 0,3I	80,0 ± 30,0			/7/
	2I2,75 ± 0,II	98 ± I5			/8/
	2I2,7	85,0 ± 4,0	22,8 ± I,5		/9/
	2I2,0	98,2 ± I0,0	24,8 ± I,3		/I0/
	2I4			0,32	/I3/
	2I2,0	87,65	24,25	0,32	*
I7	229,63 ± 0,I3	2,2 ± 0,5			/8/
	229,6	2,0 ± 0,I			/9/
	229,0	2,34 ± 0,I4			/I0/
	229,0	2,0I	22,77	0,354	*
I8	243,0	0,3 ± 0,I5			/I0/
	243,0	0,30	22,77	0,354	*
I9	280 ± 0,35	I00,0±50,0			/7/
	272,93 ± 0,I2	38 ± 5			/8/
	272,8	3I ± I,5	23,5 ± I,8		/9/
	272,4	55,0 ± I5,0	2I,5 ± 2,7		/I0/
	272,4			0,40	/I3/

I	2	3	4	5	6
	272,4	3I,58	24,45	0,40	*
20	288,68 ± 0,I3	I4,3 ± I,I			/8/
	288,6	II,5 ± I,0	25,0 ± 8,5		/9/
	288,2	I3,5 ± 2,0			/I0/
	288,2			0,48	/I3/
	288,2	I2,77	20,56	0,48	*
2I	308 ± 0,37	I30,0 ± 70,0			/7/
	303,I5 ± 0,I4	8I ± 6			/8/
	303,I	77,0 ± 3,0	22,0 ± I,5		/9/
	302,5	83,5 ± I5,0	25,8 ± I,6		/I0/
	302,5			0,46	/I3/
	302,5	77,67	23,72	0,46	*
22	320,50 ± 0,20	5,5 ± I,I			/8/
	320,5	5,4 ± 0,3			/9/
	320,0	5,8 ± 0,6			/I0/
	320,0	5,4I	22,77	0,354	*
23	334,96 ± 0,22	6,4 ± I,I			/8/
	334,9	6,2 ± 0,4			/9/
	334,4	6,3 ± 0,4			/I0/
	334,4	6,22	22,77	0,354	*
24	357,05 ± 0,30	0,70 ± 0,25			/8/
	357				/9/
	356,0	0,64 ± 0,I			/I0/
	356,0	0,70	22,77	0,354	*
25	366,95 ± 0,30	0,40 ± 0,30			/8/
	367,8	0,4 ± 0,3			/I0/
	367,8	0,40	22,77	0,354	*
26	37I,I8 ± 0,I8	I5,8 ± 2,2			/8/
	37I,2	I3,5 ± I,5	24,0 ± 4,7		/9/
	37I,0	I3,8 ± I,0			/I0/
	37I			0,42	/I3/
	37I,0	I4,23	2I,99	0,42	*
27	384 ± 0,4I	I90,0 ± I00,0			/7/
	379,8I ± 0,I9	II5 ± 24			/8/
	379,8	9I ± 4	22,0 ± I,5		/9/
	379,3	I30,0 ± 30,0	24,8 ± 3,0		/I0/

Table 1.1. (cont.)

I	2	3	4	5	6
	379				/I3/
	379,3	92,54	22,78	0,30	"
28	4I5,39 ± 0,2I	I7,7 ± 2,0			/8/
	4I5,4	I5,7 ± 0,6	22,0 ± 4,5		/9/
	4I5,0	I7,8 ± 2,0			/I0/
	4I5			0,59	/I3/
	4I5,0	I5,87	2I,67	0,59	"
29	430,95 ± 0,22	65 ± 8			/8/
	430,9	60 ± 2,5	22,0 ± I,5		/9/
	430,9	60,44	2I,94	0,354	"
30	440,63 ± 0,23	68 ± 9			/8/
	440,6	62 ± 2,5	24 ± I,6		/9/
	440,6	62,43	23,94	0,354	"
3I	465,50 ± 0,25	I5,4 ± 2,0			/8/
	465,5	I3,9 ± 0,7	22,0 ± I,5		/9/
	465,5	I4,06	2I,6I	0,354	
32	478,39 ± 0,26	40 ± 3			/8/
	478,4	37 ± 2,0	2I,0 ± I,5		/9/
	478,4	37,92	20,7I	0,354	
33	500,4I ± 0,40	2,8 ± 0,9			/8/
	500,3	2,4 ± 0,4			/9/
	500,4	2,47	22,77	0,354	
34	507,06 ± 0,28	20 ± 3			/8/
	507,I	I9 ± I	22,0 ± 3,4		"
	507,I	I9,I0	2I,87	0,354	"
35	536,37 ± 0,3I	33 ± 3			"
	536,5	30 ± 3	22,0 ± 2,4		"
	536,4	3I,50	2I,26	0,354	"
36	542,82 ± 0,44	I2,6 ± 2,4			"
	542,9	I0,3 ± 0,5	30,0 ± 8,8		"
	542,9	I0,40	29,I8	0,354	"
37	563,76 ± 0,33	8I ± 7			"
	563,8	80 ± 4	22,0 ± I,5		"
	563,8	80,25	2I,98	0,354	"
38	576,23 ± 0,34	I58 ± 25			"
	576,2	I42 ± I0	26,0 ± I,8		"
	576,2	I44,2I	25,93	0,354	/8/
39	607,I0 ± 0,43	I3 ± 2			"
	607,0	I3,3 ± 0,7	20,0 ± 8,2		"
	607,I	I3,27	20,07	0,354	"
40	6I7,80 ± 0,38	53 ± 7			"
	6I7,8	52 ± 5	24,0 ± I,8		"
	6I7,8	52,34	23,93	0,354	"
4I	637,77 ± 0,39	74 ± 8			"
	637,9	78 ± 8	24,0 ± I,8		"
	637,8	76,00	24,20	0,354	"
42	647,60 ± 0,57	7 ± 3			"
	647,I	6 ± I			"
	647,6	6,I0	22,77	0,354	"
43	655,63 ± 0,4I	I0I ± I0			"
	655,6	96 ± 8	23,0 ± I,9		"
	655,6	97,95	22,89	0,354	"
44	673,63 ± 0,43	59 ± 7			"
	673,7	54,5 ± 5	24,0 ± 2,4		"
	673,6	56,02	23,72	0,354	"
45	69I,32 ± 0,44	38 ± 4			"
	69I,3	32 ± I	27,0 ± 3,4		"
	69I,3	32,35	26,76	0,354	"
46	706,02 ± 0,45	32 ± 4			"
	706,I	28,7 ± I	2I,0 ± 2,4		"
	706,0	28,89	20,90	0,354	"
47	720,58 ± 0,47	I05 ± I0			"
	720,7	97 ± 3	2I,0 ± I,5		"
	720,6	97,66	20,97	0,354	"
48	746,25 ± 0,49	24 ± 3			"
	746,5	20,4 ± I,0	I8,0 ± 2,4		"
	746,25	20,76	I7,73	0,354	"
49	770,65 ± 0,52	I92 ± I9			"
	770,9	I8I ± I5	22,0 ± I,5		"
	770,65	I85,22	2I,94	0,354	"
50	789,43 ± 0,53	87 ± II			"
	789,6	85 ± 6	23,0 ± I,9		"
	789,4	85,46	22,97	0,354	"

Table 1.1. (cont.)

I	2	3	4	5	6
51	806,56 ± 0,55	42 ± 6			/8/
	806,5	38,6 ± I,6	24,0 ± 2,4		"
	806,6	38,83	23,9I	0,354	"
52	820,26 ± 0,8I	8,4 ± 3,6			"
	820,0	9 ± I			"
	820,3	8,96	22,77	0,354	"
53	827,43 ± 0,57	259 ± 50			"
	827,4	237 ± 20	28 ± 2		"
	827,4	240,03	27,96	0,354	"
54	849,04 ± 0,85	4 ± 2			"
	848,2	2 ± 2			"
	849,0	3,00	22,77	0,354	"
55	864,90 ± 0,87	I8 ± 6			"
	865,I	I7 ± I	I9,0 ± 2,6		"
	864,9	I7,03	I8,96	0,354	"
56	888,84 ± 0,5I	I0 ± 3			"
	888,3	7,5 ± I			"
	888,8	7,75	22,77	0,354	"
57	900,35 ± 0,65	9 ± 3			"
	900,I	4,4 ± I,0			"
	900,35	4,86	22,77	0,354	"
58	930,74 ± 0,54	II ± 3			"
	930,4	6 ± 2			"
	930,7	7,54	22,77	0,354	"
59	948,42 ± 0,43	I70 ± I5			"
	948,6	I62 ± 6	24,0 ± I,9		"
	948,4	I63,I0	23,98	0,354	"
60	955,20 ± 0,56	40 ± 5			"
	955,2	35 ± 5			"
	955,2	37,50	22,77	0,354	"
6I	969,28 ± 0,44	359 ± 47			"
	969,4	300 ± 20	23,0 ± 2,3		"
	969,3	309,05	22,95	0,354	"
62	994,70 ± 0,46	I53 ± I2			"
	994,7	I50 ± I5	22,0 ± I,7		"
	994,7	I5I,83	2I,96	0,354	"
63	998,I3 ± 0,60	II ± 3			/8/
	998				"
	998,I	II,00	22,77	0,354	"
64	I0I3,I0 ± 0,6I	II ± 4			"
	I0I3	I6,0 ± I,5			"
	I0I3,I	I5,38	22,77	0,354	"
65	I024,I9 ± 0,48	298 ± 37			"
	I024	237 ± I5	26,5 ± 2,5		"
	I024,2	245,6I	26,40	0,354	"
66	I032,I0 ± 0,63	43 ± 5			"
	I032	29,5 ± 6,0	28,0 ± 6,3		"
	I032,I	37,47	23,30	0,354	"
67	I064,62 ± 0,50	43 ± 5			"
	I065	35 ± 2	29,0 ± 6,2		"
	I064,6	36,I0	28,29	0,354	
68	I075,7I ± 0,67	6 ± 3			"
	I075	I3 ± 3			"
	I075,7	9,00	22,77	0,354	
69	I084,22 ± 0,80	2 ± I			"
	I084				"
	I084,2	2,00	22,77	0,354	
70	I098,00 ± 0,80	3 ± 2			"
	I098				"
	I098,0	3,00	22,77	0,354	
7I	II04,75 ± 0,53	I24 ± II			"
	II04	I22 ± I5	25,0 ± 2,3		"
	II04,7	I23,30	24,95	0,354	
72	II32,I0 ± 0,72	II ± 5			"
	II32	II,5 ± 2			"
	II32,I	II,43	22,77	0,354	

* Results of the present evaluation

Table 1.2. Experimental values for ^{236}U thermal cross-sections.

Reference	σ_t, 10^{-28} м^2	σ_a, 10^{-28} м^2	σ_n, 10^{-28} м^2
/12/	18,7 ± 1,7	-	-
/14/	-	5,0 ± 2,0	-
/15/	-	5,5 ± 0,3	-
/16/	-	6,0 ± 1,0	-
/10/	-	5,10 ± 0,25	-
/17/	-	5,00 ± 0,14	-
Present evaluation	18,58 ± 1,50	5,07 ± 0,15	13,51 ± 1,0

Table 1.3. Experimental values for ^{236}U capture resonance integrals.

Reference	$I_\gamma^{0,5}$, eV 10^{-28} м^2
/14/	381 ± 20
/15/	397 ± 34
/16/	450 ± 30
/17/	340 ± 15
Present evaluation	330 ± 33

Table 1.4. Evaluated neutron cross-section values for ^{236}U in the energy range 10^{-5}–10 eV at zero temperature of the sample.

E, eV	$\sigma_{n\gamma}$, 10^{-28} м^2	σ_{nn}, 10^{-28} м^2	σ_{nf}, 10^{-28} м^2
1	2	3	4
10^{-5}	250,960	13,548	3,423
$2 \cdot 10^{-5}$	177,455	13,548	2,241
$4 \cdot 10^{-5}$	125,480	13,548	1,712
10^{-4}	79,361	13,548	1,082
$2 \cdot 10^{-4}$	56,117	13,548	0,765
$4 \cdot 10^{-4}$	39,681	13,548	0,541
10^{-3}	25,098	13,547	0,342
$2 \cdot 10^{-3}$	17,748	13,546	0,242
$4 \cdot 10^{-3}$	12,552	13,543	0,171
10^{-2}	7,943	13,534	0,108
$2 \cdot 10^{-2}$	5,621	13,520	0,077
0,0253	5,000	13,512	0,068
$5 \cdot 10^{-2}$	3,565	13,477	0,049
0,1	2,533	13,407	0,034
0,2	1,811	13,271	0,024
0,5	1,200	12,888	0,016
1,0	0,952	12,318	0,012
1,5	0,914	11,803	0,011

Table 1.4. (cont.)

I	2	3	4
2,0	0,977	II,3I3	0,0I2
2,5	I,I4I	I0,8I6	0,0I4
3,0	I,454	I0,273	0,0I7
3,5	2,058	9,6I6	0,024
4,0	3,378	8,708	0,039
4,2	4,373	8,209	0,05I
4,4	5,959	7,573	0,069
4,6	8,7I2	6,722	0,I0I
4,8	I4,I49	5,508	0,I64
5,0	27,427	3,64I	0,3I8
5,I	42,82I	2,323	0,497
5,2	76,579	0,776	0,889
5,3	I76,I25	0,22I	2,043
5,35	32I,434	3,306	3,729
5,40	763,85I	2I,7I6	8,86I
5,43	I666,7I4	72,879	I9,334
5,46	5788,496	360,945	67,I47
5,49	33472,370	2822,987	388,279
5,52	5756,426	63I,42I	66,775
5,55	I648,5I0	228,203	I9,I23
5,58	75I,396	I28,I70	8,7I6
5,65	240,0I4	62,I47	2,784
5,70	I39,I59	46,420	I,6I4
5,8	63,476	32,50I	0,737
5,9	36,028	26,293	0,4I8
6,0	23,II4	22,823	0,268
6,2	II,756	I9,092	0,I37
6,4	7,06I	I7,I22	0,082
6,6	4,686	I5,900	0,055
6,8	3,325	I5,063	0,039
7,0	2,476	I4,45I	0,029
7,5	I,365	I3,446	0,0I6
8,0	0,860	I2,824	0,0I0
8,5	0,590	I2,390	0,007
9,0	0,429	I2,064	0,005
9,5	0,327	II,806	0,004
I0,0	0,258	II,594	0,003

Table 1.5. Evaluated neutron cross-sections for ^{236}U in the energy range 4-8 eV at room temperature of the sample (T = 293 K)

E, eV	$\sigma_{n\gamma}$, 10^{-28} м^2	σ_{nn}, 10^{-28} м^2	σ_{nf}, 10^{-28} м^2
I	2	3	4
4,0	3,380	8,707	0,040
4,2	4,380	8,207	0,05I
4,4	5,97I	7,57I	0,070
4,6	8,744	6,7I7	0,I02
4,8	I4,24I	5,499	0,I65
5,0	27,799	3,626	0,323
5,I	43,94I	2,257	0,5I0
5,2	80,066	0,75I	0,929
5,3	I96,I64	0,902	2,276

Table 1.5. (cont.)

I	2	3	4
5,35	405,647	7,827	4,706
5,40	I549,024	80,226	I7,969
5,43	4395,332	30I,090	50,986
5,46	9536,539	745,2I3	II0,624
5,49	I2538,980	I064,584	I45,452
5,52	9465,898	873,I43	I09,805
5,55	4384,0I2	458,553	50,855
5,58	I563,238	203,895	I8,I34
5,65	3I4,093	70,888	3,644
5,7	I58,II4	49,I09	I,843
5,8	67,305	33,22I	0,78I
5,9	37,379	26,6I9	0,434
6,0	23,462	22,90I	0,272
6,2	II,850	I9,II9	0,I38
6,4	7,095	I7,I34	0,083
6,6	4,702	I5,906	0,055
6,8	3,334	I5,067	0,039
7,0	2,48I	I4,453	0,029
7,5	I,367	I3,447	0,0I6
8,0	0,860	I2,825	0,0I0

Note: In the ranges up to 4 eV and from 8 to 10 eV the cross-sections at T = 293 K coincide with the values quoted in Table 1.4.

Table 2.1. Radiative capture cross-sections measured in Ref. [10].

E, keV	$\sigma_{n\gamma}$, 10^{-28} м^2	E,	$\sigma_{n\gamma}$, 10^{-28} м^2
0,55	5,6	3,6	I,64
0,68	6,2	4,4	I,58
0,8I	4,05	5,4	I,5
I,03	4,0	6,8	I,2
I,26	2,88	8,4	I,I6
I,58	2,6	I0,6	0,96
I,9	2,3	I3	0,94
2,35	2,04	I6	0,90
2,9I	I,8	20	0,8I

Table 2.2. Data from Ref. [19] for $\bar{\sigma}_{n\gamma}$ (^{236}U)

Δ E, keV	$\bar{\sigma}_{n\gamma}$, 10^{-28} м^2	Δ E, keV	$\bar{\sigma}_{n\gamma}$, 10^{-28} м^2
0,I0 - 0,I5	9,797 ± 2,2 *	4 - 5	I,277 ± I,9
0,I5 - 0,25	6,746 ± I,9	5 - 6	I,I54 ± 2,I
0,25 - 0,3	5,694 ± I,7	6 - 7	I,050 ± 2,7
0,3 - 0,4	5,360 ± I,6	7 - 8	0,9759 ± 2,8
0,4 - 0,5	5,I96 ± I,6	8 - 9	0,9088 ± 2,8
0,5 - 0,6	5,02I ± I,7	9 - I0	0,8925 ± 2,8
0,6 - 0,7	4,794 ± I,7	I0 - I5	0,7995 ± 2,0
0,7 - 0,8	4,238 ± I,8	I5 - 20	0,6685 ± 2,4
0,8 - 0,9	3,686 ± I,8	20 - 25	0,5832 ± 3,2
0,9 - I,0	3,423 ± I,8	25 - 30	0,5724 ± 3,2
I - 2	2,475 ± I,5	30 - 40	0,4977 ± 3,2
2 - 3	I,695 ± I,7	40 - 50	0,4276 ± 3,4
3 - 4	I,396 ± 2,0		

* Values for errors are given in percent.

Table 2.3. Data from Ref. [20] for $\sigma_{n\gamma}$

E, keV	$\sigma_{n\gamma}$, 10^{-31} м^2	E, keV	$\sigma_{n\gamma}$, 10^{-31} м^2	E, keV	σ_{γ}, 10^{-31} м^2
I2 - I4	876 ± 46	70 - 75	342 ± I6	2I0 - 220	203 ± I0
I4 - I6	873 ± 45	75 - 80	330 ± I5	220 - 230	2I3 ± I0
I6 - I8	768 ± 38	80 - 85	3I5 ± I4	230 - 240	2I4 ± I0
I8 - 20	733 ± 35	85 - 90	299 ± I3	240 - 250	I94 ± I0
20 - 22	694 ± 33	90 - 95	288 ± I3	250 - 260	I96 ± 9
22 - 24	705 ± 33	95 - I00	277 ± I2	260 - 270	202 ± 9
24 - 26	675 ± 32	I00 - II0	272 ± I2	270 - 280	I97 ± 9
26 - 28	620 ± 29	II0 - I20	257 ± I2	280 - 290	I92 ± 9
28 - 30	6I9 ± 29	I20 - I30	243 ± II	290 - 300	20I ± 9
30 - 35	585 ± 27	I30 - I40	238 ± II	300 - 320	203 ± I0
35 - 40	545 ± 25	I40 - I50	223 ± I0	320 - 340	I97 ± 9
40 - 45	53I ± 24	I50 - I60	2I4 ± I0	340 - 360	I90 ± 9
45 - 50	490 ± 23	I60 - I70	209 ± I0	360 - 380	I86 ± 9
50 - 55	433 ± 20	I70 - I80	2I6 ± I0	380 - 400	I86 ± 9
55 - 60	4I7 ± I9	I80 - I90	2I4 ± I0	400 - 420	I85 ± 9
60 - 65	389 ± I9	I90 - 200	2II ± I0		
65 - 70	358 ± I7	200 - 2I0	206 ± I0		

Table 2.4. Data from Ref. [22] for $\sigma_{n\gamma}$

E, keV	$\sigma_{n\gamma}$, 10^{-31} м^2		E, keV	$\sigma_{n\gamma}$, 10^{-31} м^2	
	Relatively $\sigma_{n\gamma}$ (^{197}Au)	Relatively σ (n,p)		Relatively $\sigma_{n\gamma}$ (^{197}Au)	Relatively σ (n,p)
I66±37	223 ± I0,7*	-	459±36	I53 ± 6,8	-
I68±35	2I3 ± I0,7	254 ± 4,I	55I±5I	I6I ± 5,I	I58 ± 3,6
I74±30	208 ± I0,7	25I ± 4,I	7I8±44	I77 ± 5,I	-
206±26	205 ± 7,I	-	890±43	I63 ± 5,I	I78 ± 3,5
240±24	I94 ± 7,I	-	I046±45	I49 ± 7,7	I53 ± 3,6
354±4I	I74 ± 6,9	I88 ± 3,8	II46±38	I26 ± 7,7	I32 ± 3,6

* Error given in percent.

Table 2.5. Mean level spacings for the ^{237}U nucleus.

E^*, keV	$D_{1/2}$, eV	$D_{3/2}$, eV	$D_{5/2}$, eV
I	I4,I05	7,329	5,209
I,5	I4,09I	7,322	5,204
2	I4,077	7,3I4	5,I99
2,5	I4,063	7,307	5,I94
3	I4,049	7,300	5,I88
4	I4,020	7,285	5,I78
6	I3,964	7,256	5,I57
8	I3,908	7,227	5,I36
I0	I3,853	7,I98	5,II6
I2	I3,797	7,I69	5,095
I4	I3,742	7,I40	5,075
I6	I3,687	7,II2	5,054
20	I3,578	7,055	5,0I4
24	I3,470	6,998	4,974
28	I3,363	6,942	4,934
32	I3,256	6,887	4,894
36	I3,I5I	6,832	4,855
40	I3,046	6,778	4,8I6
45	I2,9I6	6,7I0	4,768
50	I2,788	6,643	4,720
60	I2,535	6,5I2	4,627
70	I2,288	6,383	4,535
80	I2,045	6,257	4,445
90	II,808	6,I33	4,357
I00	II,575	6,0I2	4,26I
II0	II,347	5,894	4,I86
I20	II,I24	5,778	4,I03
I30	I0,906	5,664	4,022
I40	I0,692	5,552	3,943
I50	I0,482	5,443	3,865

* Energy reckoned from the neutron binding energy (5.125 MeV).

Table 2.6. Mean neutron widths for ^{236}U.

E_n, keV	$\Gamma^0_{n\,1/2^+}$, MeV	$\Gamma^1_{n\,1/2^-}$, MeV	$\Gamma^1_{n\,3/2^-}$, MeV	$\Gamma^2_{n\,3/2^+}$, MeV	$\Gamma^2_{n\,5/2^+}$, MeV
I	5I,562	0,26I	0,I36	0,0	0,0
I,5	63,087	0,479	0,249	0,0	0,0
2,0	72,774	0,735	0,382	0,0	0,0
2,5	8I,282	I,024	0,532	0,0	0,0
3,0	88,95I	I,343	0,698	0,0	0,0
4	I02,506	2,057	I,069	0,00I	0,0
6	I25,04I	3,738	I,942	0,003	0,002
8	I43,808	5,694	2,959	0,006	0,004
I0	I60,I39	7,875	4,092	0,0I0	0,007
I2	I74,722	I0,243	5,322	0,0I6	0,0I2
I4	I87,967	I2,773	6,637	0,024	0,0I7
I6	200,I42	I5,447	8,024	0,033	0,024
20	22I,98I	2I,I4I	I0,984	0,057	0,04I
24	24I,230	27,224	I4,I44	0,089	0,063
28	256,48I	33,6I3	I7,463	0,I29	0,092
32	274,I26	40,243	20,908	0,I78	0,I27
36	288,439	47,063	24,45I	0,236	0,I68
40	30I,620	54,032	28,07I	0,303	0,2I6
45	3I6,737	62,896	32,675	0,40I	0,285
50	330,553	7I,880	37,34I	0,5I4	0,365
60	354,947	90,020	46,764	0,785	0,558
70	375,8I8	I08,I6I	56,I85	I,II7	0,794
80	393,840	I26,096	65,499	I,5II	I,073
90	409,497	I43,677	74,629	I,964	I,395
I00	423,I46	I60,798	83,5I8	2,475	I,758
II0	435,065	I77,382	92,I28	3,042	2,I6I
I20	445,476	I93,376	I00,43I	3,66I	2,600
I30	454,556	208,744	I08,408	4,330	3,075
I40	462,454	223,463	II6,048	5,045	3,583
I50	469,296	237,520	I23,343	5,804	4,I2I

Table 2.7. Mean inelastic widths for ^{236}U.

E_n, keV	$\langle\Gamma_{n'}\rangle_{1/2^+}$, MeV	$\langle\Gamma_{n'}\rangle_{1/2^-}$, MeV	$\langle\Gamma_{n'}\rangle_{3/2^-}$, MeV	$\langle\Gamma_{n'}\rangle_{3/2^+}$, MeV	$\langle\Gamma_{n'}\rangle_{5/2^+}$, MeV
45	0,0	0,0	0,0	0,0	0,0
50	0,006	2,3I2	2,403	46,978	33,380
60	0,086	II,400	II,844	79,797	56,697
70	0,299	23,295	24,202	I0I,079	7I,8I3
80	0,672	36,685	38,III	II7,403	83,405
90	I,22I	50,890	52,866	I30,739	92,873
I00	I,953	65,489	68,030	I42,0I2	I00,875
II0	2,873	80,I99	83,307	I5I,75I	I07,785
I20	3,979	94,820	98,49I	I60,290	II3,844
I30	5,270	I09,2I2	II3,436	I67,863	II9,2I4
I40	6,740	I23,273	I28,036	I74,636	I24,0I6
I50	8,383	I36,930	I42,2I4	I80,735	I28,339

Table 2.8. Average fission widths for ^{236}U.

E_n, keV	$\langle\Gamma_f\rangle_{1/2^+}$, MeV	$\langle\Gamma_f\rangle_{1/2^-}$, MeV	$\langle\Gamma_f\rangle_{3/2^+}$, MeV	$\langle\Gamma_f\rangle_{5/2^+}$, MeV
I,0	0,356	0,034	0,0I8	0,056
I,5	0,358	0,034	0,0I8	0,056
2,0	0,359	0,034	0,0I9	0,056
2,5	0,360	0,034	0,0I9	0,056
3,0	0,36I	0,034	0,0I9	0,056
4	0,363	0,034	0,0I9	0,056
6	0,367	0,035	0,0I9	0,057
8	0,37I	0,035	0,0I9	0,058
I0	0,376	0,036	0,0I9	0,058
I2	0,380	0,036	0,020	0,059
I4	0,385	0,036	0,020	0,060
I6	0,389	0,037	0,020	0,06I
20	0,399	0,038	0,02I	0,062
24	0,408	0,039	0,02I	0,064
28	0,4I8	0,040	0,022	0,065
32	0,428	0,04I	0,022	0,066
36	0,438	0,042	0,023	0,068
40	0,448	0,043	0,023	0,070
45	0,462	0,044	0,024	0,072
50	0,475	0,045	0,025	0,074
60	0,504	0,048	0,026	0,079
70	0,534	0,05I	0,028	0,083
80	0,566	0,054	0,029	0,088
90	0,60I	0,057	0,03I	0,094
I00	0,637	0,060	0,033	0,099
II0	0,675	0,064	0,035	0,I05
I20	0,7I6	0,068	0,037	0,III
I30	0,759	0,072	0,039	0,II8
I40	0,805	0,076	0,042	0,I25
I50	0,854	0,08I	0,044	0,I33

Table 2.9. Mean radiation widths $\langle \Gamma_\gamma \rangle$ for ^{236}U in the allowed resonance energy region.

E, keV	$\langle \Gamma_\gamma \rangle$, MeV	E, keV	$\langle \Gamma_\gamma \rangle$, MeV
1,0	22,77	32,0	23,07
1,5	22,78	36,0	23,10
2,0	22,78	40,0	23,14
2,5	22,79	45,0	23,19
3,0	22,79	50,0	23,24
4,0	22,80	60,0	23,33
6,0	22,82	70,0	23,43
8,0	22,84	80,0	23,52
10,0	22,86	90,0	23,62
12,0	22,87	100,0	23,72
14,0	22,89	110,0	23,81
16,0	22,91	120,0	23,91
20,0	22,95	130,0	24,01
24,0	22,99	140,0	24,10
28,0	23,03	150,0	24,20

Table 2.10. Number of degrees of freedom for the χ^2 distribution of average partial widths.

l	J	π	ν_n	$\nu_{n'}$	ν_f	ν_γ
0	1/2	+	1	2	2	
1	1/2	−	1	1	2	
1	3/2	−	1	2	4	∞
2	3/2	+	1	1	4	
2	5/2	+	1	1	6	

Table 2.11. Average neutron sections in the forbidden resonance energy region.

E, keV	σ_t, 10^{-28} м^2	σ_{nn}, 10^{-28} м^2	$\sigma_{nn'}$, 10^{-28} м^2	σ_{nf}, 10^{-28} м^2	$\sigma_{n\gamma}$, 10^{-28} м^2
1	26,564	23,202		0,049	3,313
1,5	23,809	21,272		0,035	2,502
2	22,170	20,067		0,028	2,075
2,5	21,052	19,283		0,022	1,747
3	20,227	18,633		0,020	1,574
4	19,070	17,696		0,016	1,358
6	17,696	16,596		0,011	1,089
8	16,874	15,909		0,009	0,956
10	16,311	15,417		0,008	0,886
12	15,890	15,071		0,006	0,813
14	15,561	14,768		0,006	0,787
16	15,293	14,527		0,006	0,760
20	14,876	14,181		0,005	0,690
24	14,559	13,921		0,004	0,634
28	14,304	13,721		0,004	0,579
32	14,093	13,545		0,003	0,545
36	13,913	13,389		0,003	0,521
40	13,756	13,257		0,003	0,496
45	13,584	13,100	0,0	0,003	0,481
50	13,428	12,959	0,038	0,003	0,428
60	13,184	12,666	0,146	0,002	0,370
70	12,980	12,404	0,240	0,002	0,334
80	12,819	12,184	0,332	0,002	0,301
90	12,676	11,990	0,414	0,002	0,270
100	12,578	11,828	0,495	0,002	0,253
110	12,473	11,661	0,573	0,002	0,237
120	12,373	11,513	0,632	0,002	0,226
130	12,270	11,367	0,681	0,002	0,220
140	12,171	11,240	0,717	0,002	0,212
150	12,076	11,114	0,748	0,002	0,212

Table 3.1. Evaluated errors for the fission cross-section ratio ^{236}U and ^{235}U.

Energy range, MeV	Evauated error in the ratio $\sigma_f(^{236}U)/\sigma_f(^{235}U)$, %
0,15 - 0,2	50
0,2 - 0,5	20
0,5 - 0,7	10
0,7 - 0,9	5-7
0,9 - 1,4	3-5
1,4 - 5,0	2-3
5 - 7,5	3-5
7,5 - 20	5

Table 3.2. Evaluated data for the ratio $\sigma_f(^{236}U)/\sigma_f(^{235}U)$

E, MeV	$\sigma_f(^{236}U)/\sigma_f(^{235}U)$	E, MeV	$\sigma_f(^{236}U)/\sigma_f(^{235}U)$	E, MeV	$\sigma_f(^{236}U)/\sigma_f(^{235}U)$
0,15	$1,373\cdot10^{-3}$	1,2	0,4795	12,5	0,8364
0,16	$1,389\cdot10^{-3}$	1,4	0,5876	13,0	0,7990
0,18	$1,420\cdot10^{-3}$	1,6	0,5411	13,5	0,7768
0,20	$1,452\cdot10^{-3}$	1,8	0,5986	14,0	0,7650
0,22	$1,489\cdot10^{-3}$	2,0	0,6356	14,5	0,7718
0,24	$1,522\cdot10^{-3}$	2,2	0,6767	15,0	0,7946
0,26	$1,549\cdot10^{-3}$	2,4	0,6909	15,5	0,8285
0,28	$1,572\cdot10^{-3}$	2,6	0,6958	16,0	0,8549
0,30	$1,585\cdot10^{-3}$	2,8	0,7081	16,5	0,8762
0,32	$1,598\cdot10^{-3}$	3,0	0,7219	17,0	0,9109
0,34	$1,612\cdot10^{-3}$	3,2	0,7402	17,5	0,9240
0,36	$1,627\cdot10^{-3}$	3,4	0,7525	18,0	0,9366
0,38	$1,641\cdot10^{-3}$	3,6	0,7674	18,5	0,9383
0,40	$2,481\cdot10^{-3}$	3,8	0,7779	19,0	0,9313
0,42	$2,503\cdot10^{-3}$	4,0	0,7880	19,5	0,9407
0,44	$3,365\cdot10^{-3}$	4,5	0,7858	20,0	0,9394
0,46	$3,390\cdot10^{-3}$	5,0	0,8083		
0,48	$4,264\cdot10^{-3}$	5,5	0,7937		
0,50	$5,141\cdot10^{-3}$	6,0	0,8498		
0,55	$7,792\cdot10^{-3}$	6,5	0,8556		
0,60	$1,223\cdot10^{-2}$	7,0	0,9163		
0,65	$1,930\cdot10^{-2}$	7,5	0,9139		
0,70	$3,782\cdot10^{-2}$	8,0	0,8822		
0,75	$6,860\cdot10^{-2}$	8,5	0,8822		
0,80	$1,133\cdot10^{-1}$	9,0	0,8871		
0,85	$1,595\cdot10^{-1}$	9,5	0,8876		
0,90	0,2123	10,0	0,8862		
0,95	0,2848	10,5	0,8867		
1,00	0,2984	11,0	0,8866		
1,05	0,3053	11,5	0,8833		
1,1	0,3728	12,0	0,8770		

Table 4.1.

Level No.	Level energy, keV	Spin J and parity π of the level
I	0,0	0^+
2	45,242	2^+
3	I49,475	4^+
4	309,785	6^+
5	522,25	8^+
6	687,57	I^-
7	744,20	3^-
8	782,80	$I0^+$
9	847,60	5^-
I0	9I9,I6	0^+
II	958,I0	2^+
I2	960,40	2^+
I3	967,0	I^-
I4	988,0	2^-
I5	I00I,40	3^+
I6	I002,0	7^-

Table 4.2. Evaluated data for ^{236}U neutron cross-sections in the fast neutron energy range.

E, MeV	σ_t, 10^{-28} m^2	σ_n, 10^{-28} m^2	σ_f, 10^{-28} m^2	$\sigma_{n\gamma}$, 10^{-28} m^2	$\sigma_{nn'}$, 10^{-28} m^2 direct	$\sigma_{nn'}$, 10^{-28} m^2 total	σ_{n2n}, 10^{-28} m^2	σ_{n3n}, 10^{-28} m^2
I	2	3	4	5	6		7	8
0,I6	II,525	I0,635	0,002	0,2I2	0,747	0,776		
0,I8	II,250	I0,205	0,002	0,203	0,808	0,840		
0,20	I0,955	9,874	0,002	0,I95	0,855	0,894		
0,22	I0,520	9,403	0,002	0,I93	0,878	0,922		
0,24	I0,I80	9,057	0,002	0,I90	0,880	0,93I		
0,26	9,840	8,713	0,002	0,I85	0,880	0,939		
0,28	9,594	8,462	0,002	0,I83	0,876	0,947		
0,30	9,348	8,I85	0,002	0,I79	0,907	0,982		
0,32	9,I50	7,964	0,002	0,I75	0,927	I,009		
0,34	8,990	7,775	0,002	0,I7I	0,954	I,042		
0,36	8,840	7,598	0,002	0,I68	0,977	I,072		
0,38	8,700	7,430	0,002	0,I63	I,002	I,I05		
0,40	8,566	7,269	0,003	0,I59	I,026	I,I35		
0,42	8,440	7,II4	0,003	0,I55	I,053	I,I68		
0,44	8,330	6,972	0,004	0,I52	I,08I	I,202		
0,46	8,220	6,830	0,004	0,I5I	I,I06	I,235		
0,48	8,II0	6,683	0,005	0,I5I	I,I36	I,27I		
0,50	8,032	6,572	0,006	0,I52	I,I60	I,302		
0,55	7,780	6,247	0,009	0,I57	I,2I3	I,367		
0,60	7,604	5,997	0,0I4	0,I63	I,257	I,430		
0,65	7,430	5,746	0,022	0,I68	I,306	I,494		
0,70	7,280	5,489	0,043	0,I72	I,374	I,576		
0,75	7,I50	5,2I8	0,078	0,I75	I,462	I,679		
0,80	7,053	4,984	0,I29	0,I73	I,533	I,767		
0,85	6,970	4,793	0,I83	0,I69	I,577	I,825		
0,90	6,900	4,622	0,248	0,I64	I,603	I,865		
0,95	6,840	4,452	0,342	0,I58	I,609	I,888		
I,00	6,795	4,285	0,354	0,I5I	I,702	I,996		
I,05	6,760	4,I53	0,37I	0,I42		2,094		
I,I	6,750	3,972	0,453	0,I34	I,859	2,I9I		
I,2	6,754	3,754	0,585	0,II4	I,952	2,30I		

Table 4.2. (cont.)

I	2	3	4	5	6		7	8
I,4	6,850	3,625	0,728	0,090	2,III	2,507		
I,6	7,040	3,564	0,684	0,074	2,283	2,716		
I,8	7,244	3,638	0,77I	0,062	2,305	2,773		
2,0	7,442	3,770	0,825	0,054	2,303	2,793		
2,2	7,62	3,896	0,874	0,047	2,298	2,803		
2,4	7,755	4,044	0,883	0,040	2,277	2,783		
2,6	7,859	4,187	0,876	0,034	2,25I	2,762		
2,8	7,930	4,294	0,878	0,029	2,22I	2,729		
3,0	7,985	4,382	0,880	0,024	2,195	2,699		
3,2	8,010	4,45I	0,889	0,020	2,144	2,640		
3,4	7,999	4,502	0,89I	0,016	2,10I	2,590		
3,6	7,970	4,508	0,894	0,013	2,074	2,555		
3,8	7,940	4,514	0,893	0,0II	2,052	2,522		
4,0	7,89I	4,497	0,892	0,009	2,03I	2,493		
4,5	7,7I2	4,379	0,873	0,007	2,0I5	2,453		
5,0	7,5I3	4,I98	0,860	0,006	2,006	2,424		
5,5	7,244	3,984	0,83I	0,006	2,023	2,423		
6,0	6,992	3,754	0,945	0,005	I,905	2,288		
6,5	6,745	3,525	I,I67	0,005	I,680	2,048		
7,0	6,52I	3,3I3	I,423	0,004	I,358	I,7II	0,070	
7,5	6,332	3,I38	I,57I	0,004	I,060	I,399	0,220	
8,0	6,I6I	2,98I	I,572	0,003	0,82	I,I45	0,460	
8,5	6,020	2,848	I,572	0,003	0,585	0,897	0,700	
9,0	5,9II	2,746	I,572	0,002	0,42I	0,72I	0,870	
9,5	5,828	2,675	I,564	0,002	0,35I	0,637	0,950	
I0,0	5,764	2,6I6	I,550	0,00I	0,3I9	0,597	I,000	
I0,5	5,72I	2,587	I,54I	0,00I	0,298	0,572	I,020	
II,0	5,698	2,57I	I,539	0,00I	0,270	0,547	I,040	
II,5	5,688	2,578	I,535	0,00I	0,240	0,5I8	I,056	
I2,0	5,700	2,602	I,533	0,00I	0,22I	0,499	I,065	
I2,5	5,7I9	2,638	I,53I	0,00I	0,I93	0,469	I,065	0,0I5
I3,0	5,746	2,685	I,530	0,00I	0,I76	0,448	I,045	0,037
I3,5	5,78I	2,743	I,552	0,00I	0,I63	0,43I	0,972	0,082
I4,0	5,824	2,804	I,582	0,00I	0,I52	0,4I7	0,855	0,I65
I4,5	5,857	2,86I	I,620	0,00I	0,I44	0,405	0,720	0,250
I5,0	5,895	2,922	I,67I	0,00I	0,I33	0,39I	0,580	0,330
I5,5	5,936	2,974	I,734	0,00I	0,I23	0,377	0,470	0,380
I6,0	5,978	3,037	I,768	0,00I	0,III	0,362	0,390	0,420
I6,5	6,005	3,08I	I,786	0,00I	0,I03	0,349	0,336	0,450
I7,0	6,048	3,I30	I,804	0,00I	0,095	0,338	0,295	0,480
I7,5	6,080	3,I74	I,8II	0,00I	0,090	0,329	0,260	0,505
I8,0	6,III	3,2I5	I,8I6	0,00I	0,085	0,3I9	0,240	0,520
I8,5	6,I43	3,253	I,825	0,00I	0,080	0,3I0	0,220	0,534
I9,0	6,I67	3,284	I,839	0,00I	0,075	0,302	0,205	0,536
I9,5	6,I86	3,309	I,860	0,00I	0,070	0,294	0,I90	0,532
20,0	6,I92	3,32I	I,889	0,00I	0,065	0,286	0,I75	0,520

Table 4.3. ^{236}U level excitation cross-sections

E_n, MeV	Level energy E_q, keV: 45,24 (direct excitation, 10^{-28} m^2)	149,48 (direct excitation, 10^{-28} m^2)	45,24 (Compound nucleus mechanism)	149,48 (Compound nucleus mechanism)	309,78	522,25	687,57	744,20	847,60
0,16	0,029		0,7470	0,0					
0,18	0,032		0,8074	0,0006					
0,20	0,039		0,8535	0,0015					
0,22	0,044		0,8753	0,0027					
0,24	0,051		0,8756	0,0044					
0,26	0,059		0,8736	0,0064					
0,28	0,067	0,0	0,8674	0,0126					
0,30	0,074	0,001	0,8792	0,0278					
0,32	0,080	0,002	0,8926	0,0344					
0,34	0,085	0,003	0,9122	0,0418					
0,36	0,091	0,004	0,9271	0,0499					
0,38	0,098	0,005	0,9433	0,0587					
0,40	0,103	0,006	0,9577	0,0683					
0,42	0,108	0,007	0,9743	0,0787					
0,44	0,113	0,008	0,9908	0,0902	0,0				
0,46	0,119	0,010	1,0040	0,1019	0,0001				
0,48	0,123	0,012	1,0209	0,1149	0,0002				
0,50	0,128	0,014	1,0319	0,1278	0,0003				

Table 4.3. (cont.)

E_n, MeV	Level energy E_q, keV: 45,24 (direct excitation, 10^{-28} m^2)	149,48 (direct excitation, 10^{-28} m^2)	45,24 (Compound nucleus mechanism)	149,48 (Compound nucleus mechanism)	309,78	522,25	687,57	744,20	847,60
0,55	0,136	0,018	1,0502	0,1622	0,0006				
0,60	0,150	0,023	1,0578	0,1979	0,0013				
0,65	0,159	0,029	1,0672	0,2363	0,0025		0,0		
0,70	0,168	0,034	1,0528	0,2739	0,0045		0,0428	0,0	
0,75	0,176	0,041	1,0104	0,3021	0,0068		0,1362	0,0065	
0,80	0,186	0,048	0,9514	0,3208	0,0094		0,1908	0,0506	
0,85	0,193	0,055	0,9184	0,3406	0,0128		0,2219	0,0833	0,0
0,90	0,201	0,062	0,8801	0,3584	0,0167		0,2392	0,1079	0,0007
0,95	0,210	0,069	0,8328	0,3695	0,0209		0,2422	0,1251	0,0021
1,00	0,217	0,077	0,7703	0,3737	0,0255		0,2330	0,1331	0,0040
1,05	0,225	0,083	0,7157	0,3605	0,0267		0,2173	0,1285	0,0055
1,1	0,233	0,089	0,6610	0,3473	0,0279		0,2016	0,1239	0,0071
1,2	0,247	0,102	0,5328	0,3128	0,0335	0,0	0,1669	0,1158	0,0104
1,4	0,274	0,122	0,3817	0,2571	0,0421	0,0001	0,1216	0,0994	0,0153
1,6	0,298	0,137	0,2876	0,2091	0,0451	0,0003	0,0930	0,0851	0,0180
1,8	0,320	0,148	0,2023	0,1532	0,0394	0,0004	0,0674	0,0672	0,0176
2,0	0,335	0,155	0,1385	0,1073	0,0308	0,0005	0,0481	0,0515	0,0157
2,2	0,346	0,159	0,0930	0,0731	0,0225	0,0006	0,0340	0,0383	0,0132
2,4	0,351	0,160	0,0611	0,0486	0,0157	0,0006	0,0235	0,0276	0,0105
2,6	0,352	0,159	0,0395	0,0319	0,0107	0,0005	0,0160	0,0194	0,0080

Table 4.3. (cont.)

E_n, MeV	Level energy E_q, keV: 9I9,I6	958,I0	960,40	967,00	988,00	I00I,40	I002,00	Continuous spectrum excitation, $10^{-28}\,m^2$
0,90	0,0							
0,95	0,0I64	0,0	0,0	0,0	0,0			
I,00	0,0383	0,0392	0,0367	0,0358	0,0I24	0,0		0,0
I,05	0,0484	0,0725	0,0702	0,052I	0,0336	0,0256		0,0294
I,I	0,0585	0,I057	0,I037	0,0683	0,0548	0,05I3		0,0579
I,2	0,0637	0,I404	0,I39I	0,0859	0,0735	0,09I4	0,0	0,I858
I,4	0,0572	0,I494	0,I487	0,0830	0,0804	0,II74	0,000I	0,5575
I,6	0,0474	0,I327	0,I323	0,0709	0,0737	0,II2I	0,0002	0,9755
I,8	0,0364	0,I052	0,I048	0,0543	0,0594	0,0925	0,0005	I,3044
2,0	0,0274	0,0808	0,0806	0,0402	0,0458	0,0735	0,0007	I,56I6
2,2	0,0202	0,0607	0,0606	0,0292	0,0345	0,0569	0,00I0	I,7602
2,4	0,0I43	0,0438	0,0438	0,0207	0,025I	0,042I	0,00II	I,8985
2,6	0,0097	0,0306	0,0305	0,0I44	0,0I78	0,0299	0,00I0	I,99II

Table 4.3. (cont.)

E_n, MeV	Level energy E_q, keV: 45,24	I49,48	45,24	I49,48	309,76	522,25	687,57	744,20	847,60
	direct excitation, $10^{-28}\,m^2$		Compound nucleus mechanism						
2,8	0,350	0,I58	0,0253	0,0207	0,0072	0,0005	0,0I07	0,0I33	0,0059
3,0	0,347	0,I57	0,0I60	0,0I33	0,0049	0,0004	0,007I	0,0090	0,0042
3,2	0,342	0,I54	0,0097	0,0085	0,0035	0,0004	0,0044	0,0058	0,0030
3,4	0,337	0,I52	0,0060	0,0053	0,0023	0,0004	0,0028	0,0038	0,002I
3,6	0,332	0,I49	0,0037	0,0034	0,00I5	0,0003	0,00I8	0,0025	0,00I4
3,8	0,324	0,I46	0,0023	0,0022	0,00I0	0,0002	0,00II	0,00I6	0,00I0
4,0	0,3I8	0,I44	0,00I4	0,00I4	0,0006	0,000I	0,0007	0,00I0	0,0006
4,5	0,302	0,I36	0,0	0,0	0,0	0,0	0,0	0,0	0,0

E_n, MeV	Level energy E_q, keV: 9I9,I6	958,I0	960,40	967,00	988,00	I00I,40	I002,00	Continuous spectrum excitation, $10^{-28}\,m^2$
2,8	0,0064	0,0207	0,0206	0,0098	0,0I24	0,0205	0,0009	2,0462
3,0	0,0042	0,0I36	0,0I36	0,0066	0,0084	0,0I36	0,0008	2,0793
3,2	0,0025	0,0085	0,0085	0,004I	0,0054	0,0087	0,0007	2,0703
3,4	0,00I6	0,0053	0,0053	0,0026	0,0035	0,0055	0,0006	2,0539
3,6	0,0009	0,0033	0,0033	0,00I7	0,0022	0,0035	0,0004	2,044I
3,8	0,0006	0,002I	0,002I	0,00II	0,00I4	0,0022	0,0003	2,0328
4,0	0,0004	0,00I2	0,00I2	0,0007	0,0009	0,00I4	0,0002	2,0I90
4,5	0,0	0,0	0,0	0,0	0,0	0,0	0,0	2,0I50

Table 4.3. (cont.)

E_n, MeV	E_q, keV: 45,24	E_q, keV: I49,48	Continuous spectrum excitation, 10^{-28} м^2	E_n, MeV	E_q: 45,24	E_q: I49,48	Continuous spectrum excitation, 10^{-28} м^2
	Direct excitation 10^{-28} м^2				Direct excitation 10^{-28} м^2		
5,0	0,289	0,129	2,006	I3,0	0,2II	0,06I	0,I76
5,5	0,278	0,122	2,023	I3,5	0,209	0,059	0,I63
6,0	0,268	0,II5	I,905	I4,0	0,207	0,058	0,I52
6,5	0,260	0,I08	I,680	I4,5	0,204	0,057	0,I44
7,0	0,252	0,I0I	I,358	I5,0	0,202	0,056	0,I33
7,5	0,244	0,095	I,060	I5,5	0,I99	0,055	0,I23
8,0	0,237	0,088	0,820	I6,0	0,I97	0,054	0,III
8,5	0,229	0,083	0,585	I6,5	0,I94	0,052	0,I03
9,0	0,222	0,078	0,42I	I7,0	0,I92	0,05I	0,095
9,5	0,2I3	0,073	0,35I	I7,5	0,I90	0,049	0,090
I0,0	0,209	0,069	0,3I9	I8,0	0,I87	0,047	0,085
I0,5	0,207	0,067	0,298	I8,5	0,I84	0,046	0,080
II,0	0,2II	0,066	0,270	I9,0	0,I82	0,045	0,075
II,5	0,2I3	0,065	0,240	I9,5	0,I80	0,044	0,070
I2,0	0,2I4	0,064	0,22I	20,0	0,I78	0,043	0,055
I2,5	0,2I3	0,063	0,I93				

Table 5.1. Fission barrier parameters for uranium isotopes.

Parameter	Compound nucleus: ^{237}U	^{236}U	^{235}U	^{234}U
E_A, MeV	6,2	5,7	5,8	5,7
$\hbar\omega_A$, MeV	I,2	I,2	I,2	I,2
E_B, MeV	5,85	5,55	5,75	5,50
$\hbar\omega_B$, MeV	0,5	0,6	0,5	0,60

Table 5.2. Level density parameters for uranium isotopes.

Parameter	Compound nucleus: ^{236}U	^{235}U	^{234}U
I^{π}	$7/2^-$	0^+	$5/2^+$
B_n, MeV	6,546	5,305	6,84I
T_n, MeV	0,383	0,40I	0,392
E_o, MeV	0,0I56	– 0,934I	0,0I86
U_c, MeV	4,I	3,8	4,0
$\sigma^2_{I\,exp}$	II,25	I2,22	II,35
<D> [?]	0,438±0,038	I0,6± 0,5	0,6I ± 0,07
δW_{exp} MeV	– I,624	– I,700	– I,704
$\tilde{a}$, MeV^{-I}	24,863	23,500	2I,986
$a(B_n)$, MeV^{-I}	22,6I4	2I,25I	I9,933

Table 6.1. Average number of neutrons emitted per fission event.

E, MeV	$\bar{\nu}_p$	$\bar{\nu}_t$	$\Delta\bar{\nu}_t$	E, MeV	$\bar{\nu}_p$	$\bar{\nu}_t$	$\Delta\bar{\nu}_t$
10^{-5}	2,348	2,374	0,030	4,0	2,860	2,886	0,022
0,1	2,360	2,386	0,030	6,0	3,150	3,171	0,025
0,2	2,371	2,397	0,030	8,0	3,412	3,428	0,050
0,3	2,383	2,409	0,030	10,0	3,674	3,690	0,060
0,4	2,394	2,420	0,030	12,0	3,936	3,952	0,070
0,5	2,406	2,432	0,028	14,7	4,289	4,305	0,080
0,6	2,417	2,443	0,026	16,0	4,442	4,458	0,100
0,7	2,429	2,455	0,024	18,0	4,678	4,694	0,120
0,8	2,441	2,467	0,022	20,0	4,913	4,929	0,120
1,0	2,464	2,490	0,019				
1,5	2,522	2,548	0,019				
2,0	2,579	2,605	0,019				
2,35	2,620	2,646	0,019				
3,0	2,714	2,740	0,019				

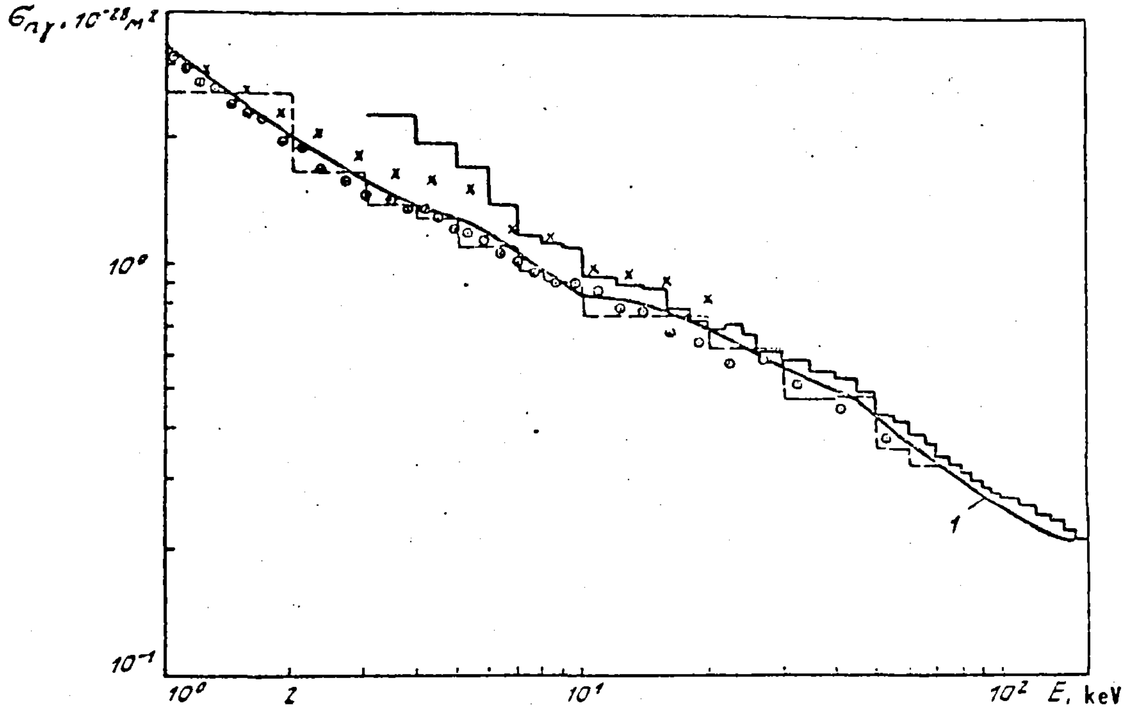

Fig. 2.1. Comparison of evaluated (1) and experimental data for $\sigma_{n\gamma}(^{236}U)$ in the 1-150 keV energy range.

o - /19/; x - /10/; ⅂ - /20/; ‾⅂_ - /72/

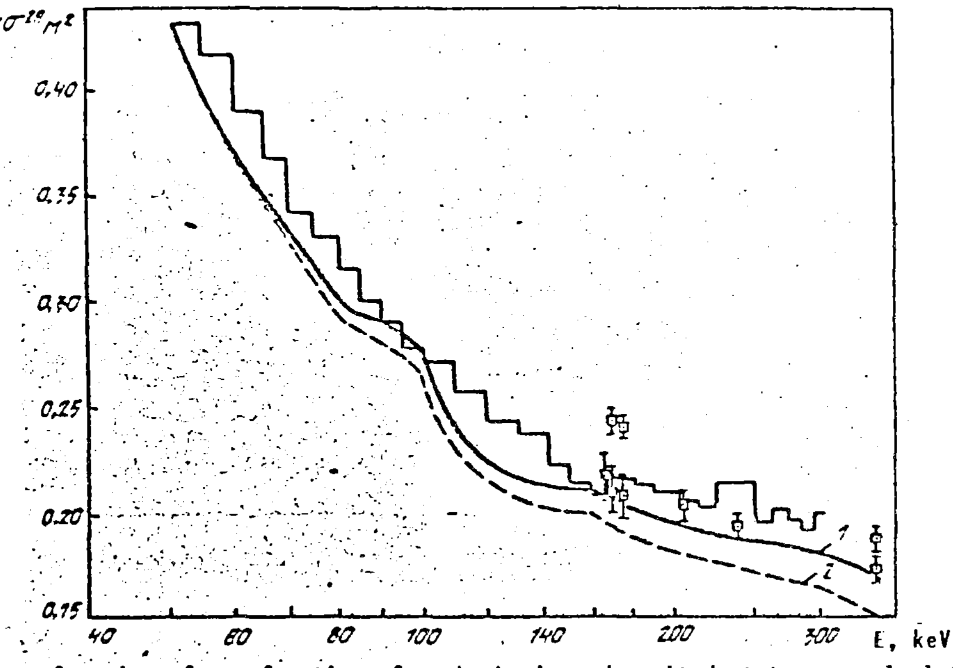

Fig. 2.2. Effects of various force functions for the basic and excited states on calculation of $\sigma_{n\gamma}$:
1 – Calculation taking account of the difference in S_0 in the ground and excited states;
2 – Without allowing for this difference; [20]; [22] (experimental data).

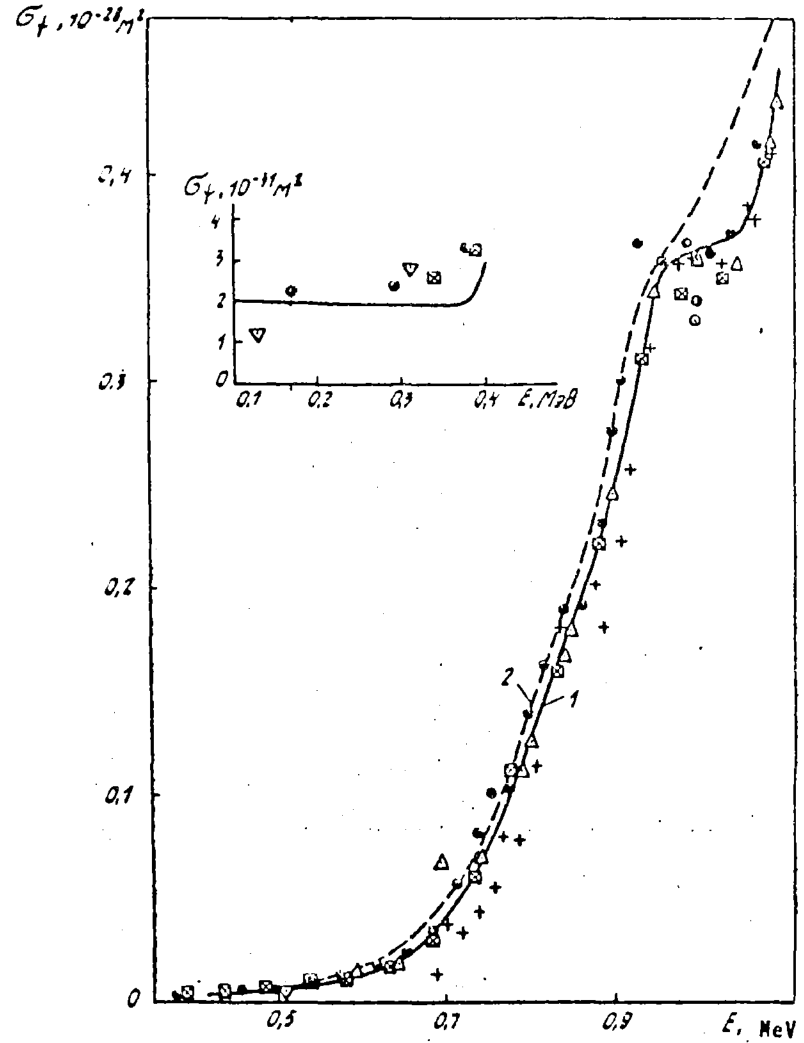

Fig. 3.1. Comparison of evaluated and experimental data for σ_f in the energy range 0.1–1.1 MeV:
1 – result of the present evaluation; 2 – ENDF/B-V evaluation [63];
● – /32/; ⊠ – /36/; △ – /34/; + – /30/; ⊙ – /31/;
o – /29/

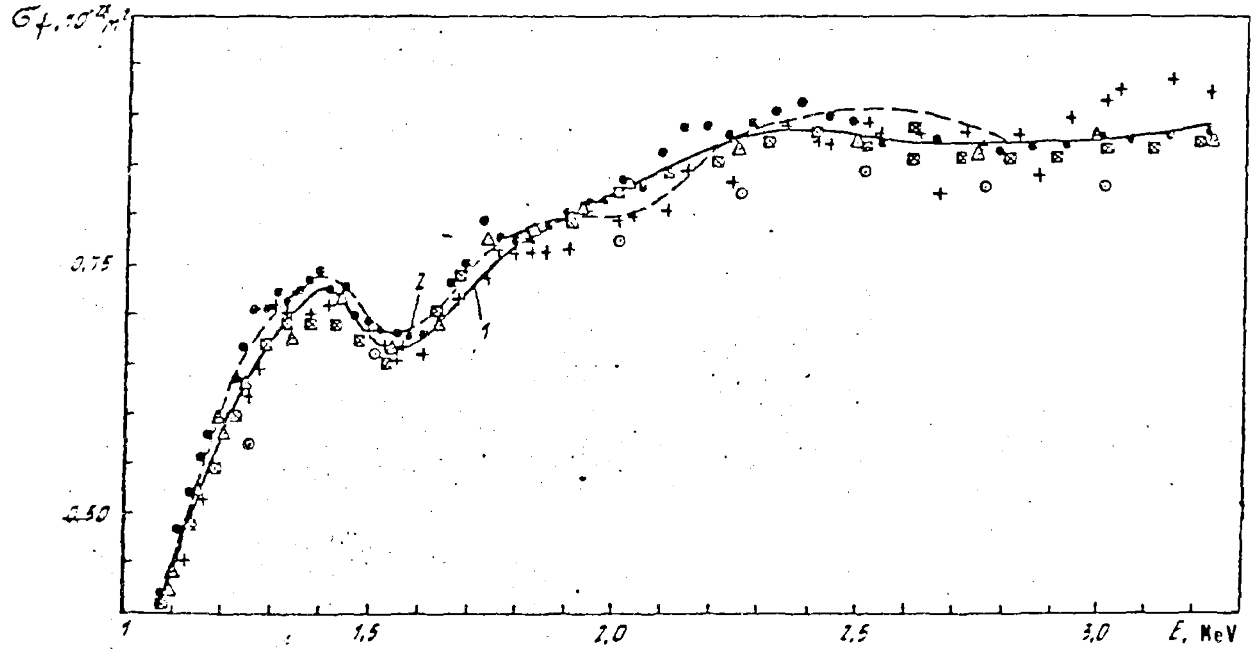

Fig. 3.2. Comparison of evaluated and experimental data for σ_χ in the 1–3 MeV range: 1 – result of the present evaluation; 2 – ENDF/B-V evaluation [63]; • – [32]; ⊠ – [36]; △ – [34]; + – [30]; ⊙ – [31].

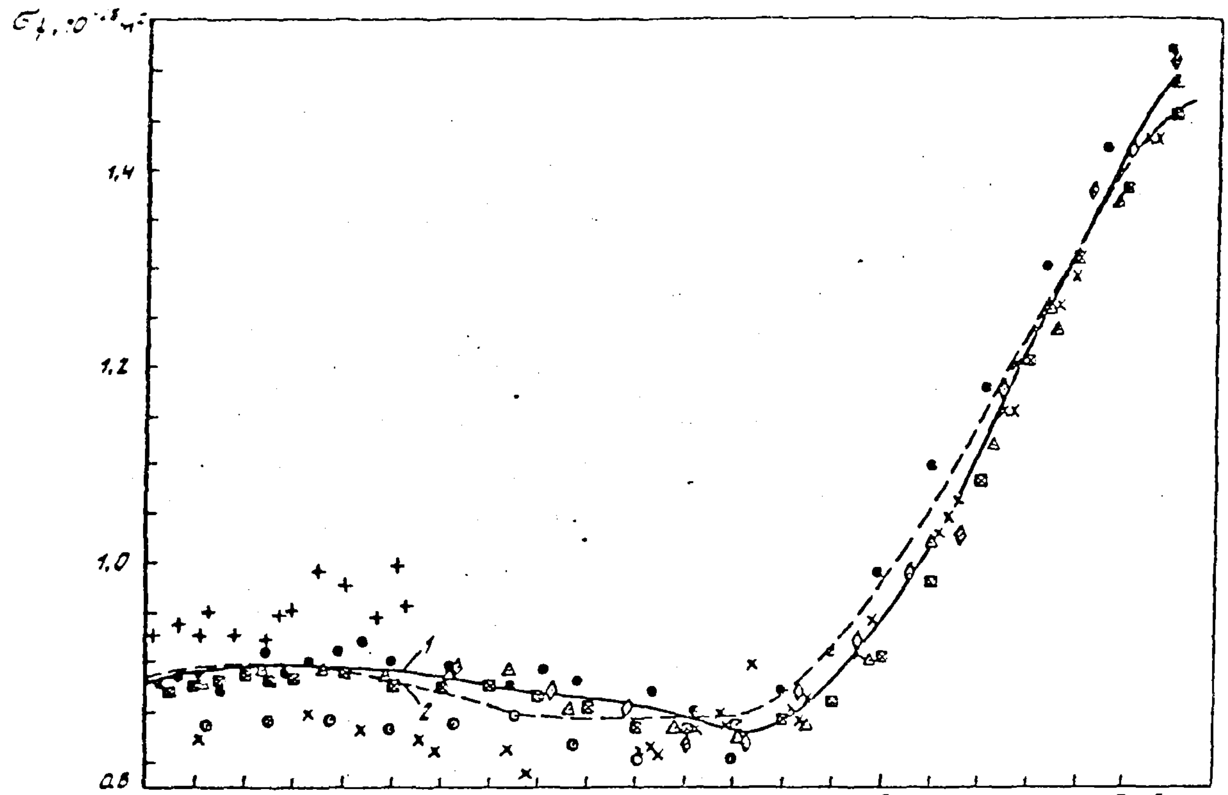

Fig. 3.3. Comparison of evaluated and experimental data for σ_χ in the 3–7 MeV range:
1 – result of the present evaluation; 2 – ENDF/B-V evaluation [63]; • – [32]; ⊠ – [36]; △ – [34]; + – [30]; x – [33]; ⊖ – [31]; ◇ – [35].

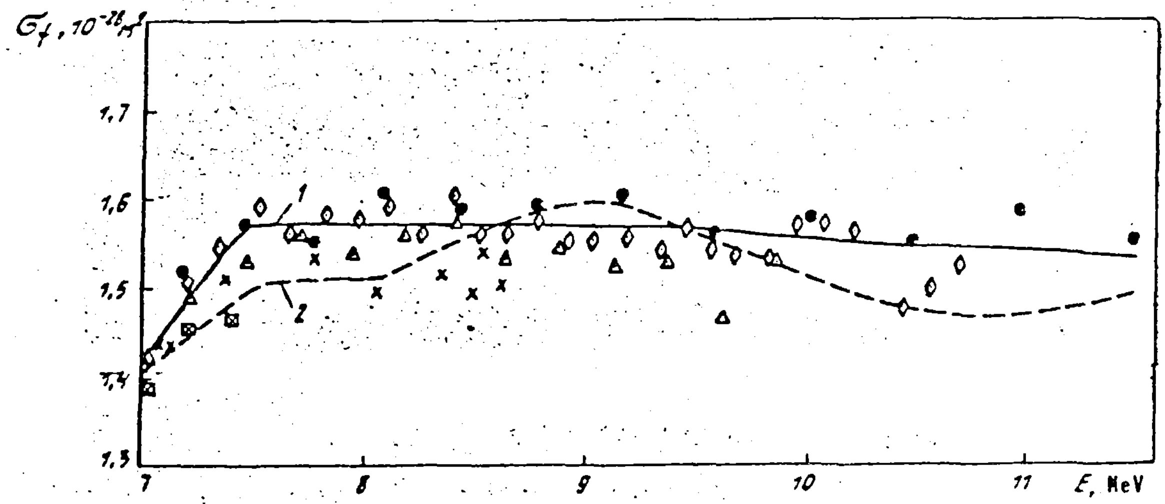

Fig. 3.4. Comparison of evaluated and experimental data for σ_{χ} in the 7-11 MeV range; 1 - result of the present evaluation; 2 - ENDF/B-V evaluation [63]; • - [32]; x - [33]; ⊠ - [36]; ◇ - [35]; △ - [34].

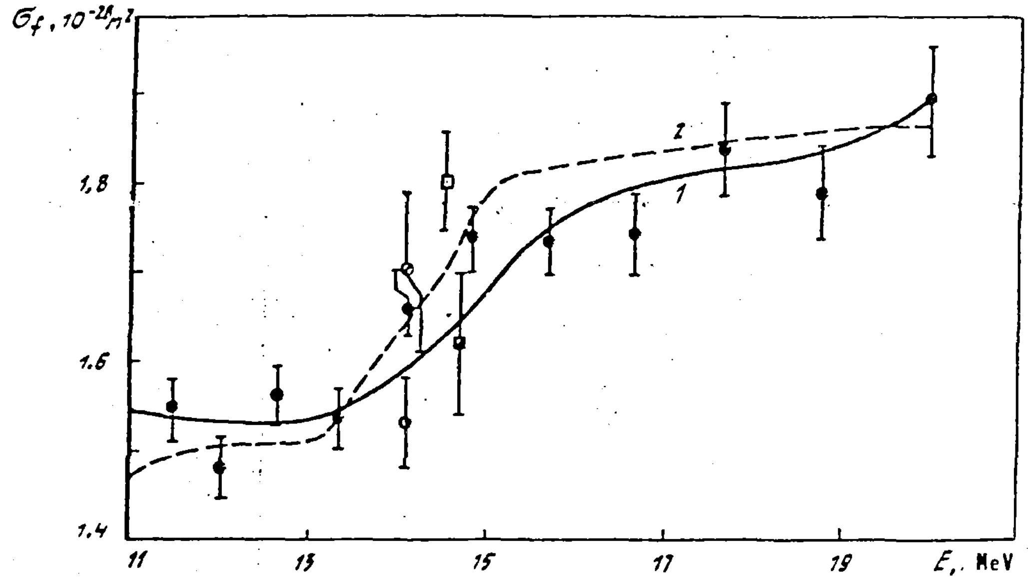

Fig. 3.5. Comparison of evaluated and experimental data for σ_{χ} in the 7-11 MeV range; 1 - result of the present evaluation; 2 - ENDF/B-V evaluation [63]; ⧳ - [32]; ⊕ - [29]; ⧄ - [39]; ⊘ - [38]; ⊡ - [37].

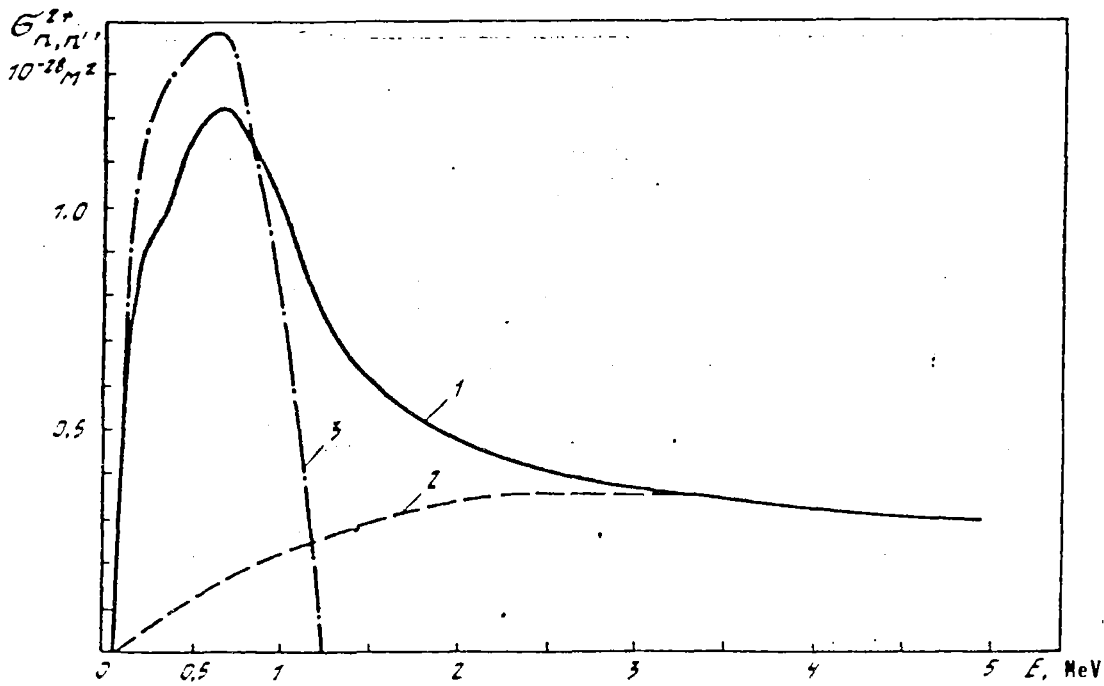

Fig. 4.1. Level 2^+ (45.24 keV) excitation cross-section: 1 - Total excitation cross-section; 2 - excitation cross-section for the direct process (results of the present evaluation); 3 - ENDF/B-V evaluation [63].

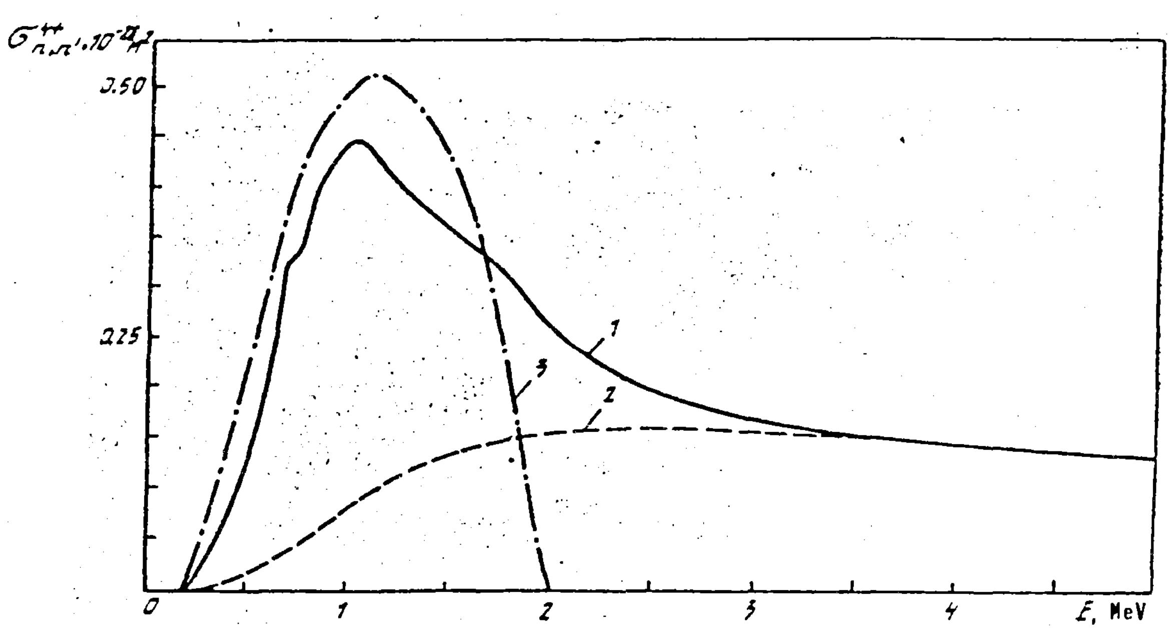

Fig. 4.2. Level 4^+ (149.48 keV) excitation cross-section: 1 - Total excitation cross-section; 2 - Excitation cross-section for the direct process (results of the present evaluation); 3 - ENDF/B-V evaluation [63].

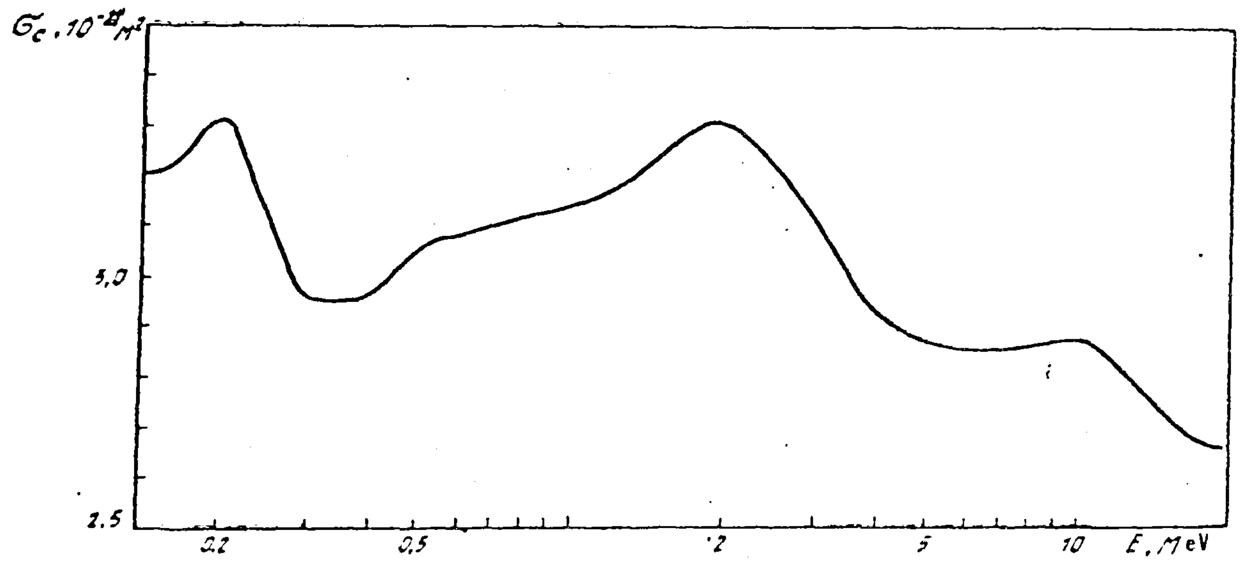

Fig. 4.3. Cross-section for formation of the ^{237}U compound nucleus (calculated by the coupled-channel method).

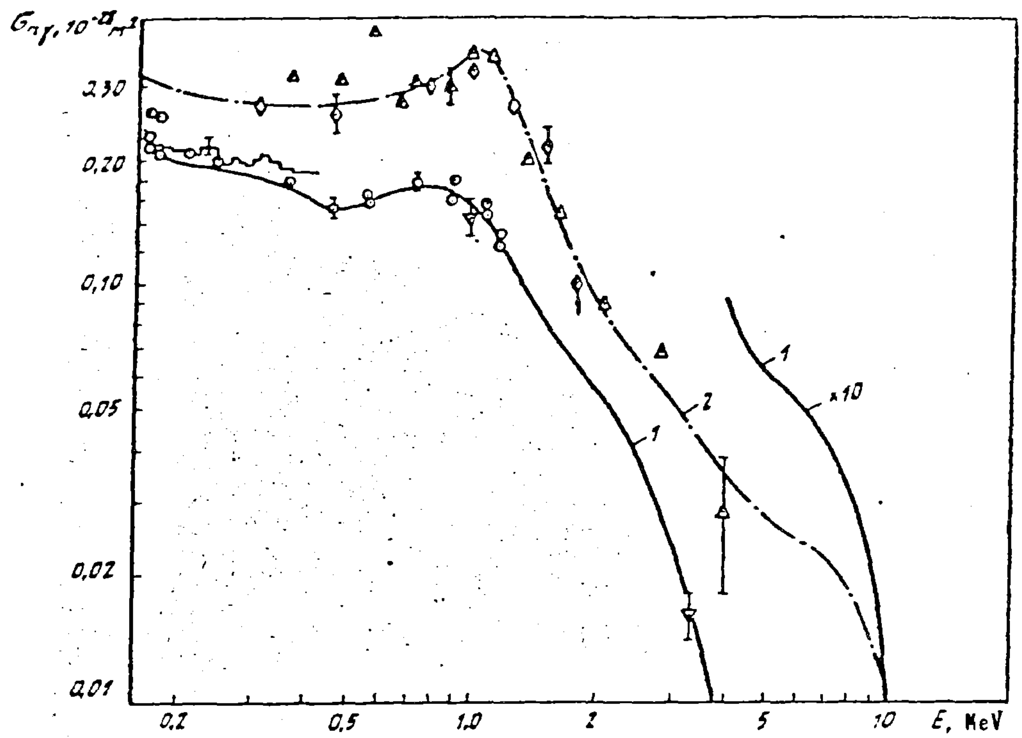

Fig. 4.4. Comparison of evaluated and experimental data for $\sigma_{n\gamma}$ ^{236}U :
1 - present evaluation; 2 - ENDF/B-V evaluation [63]; – [20]; e - [22];
△ - [56]; ◇ - [57]; ⊽ - [56].

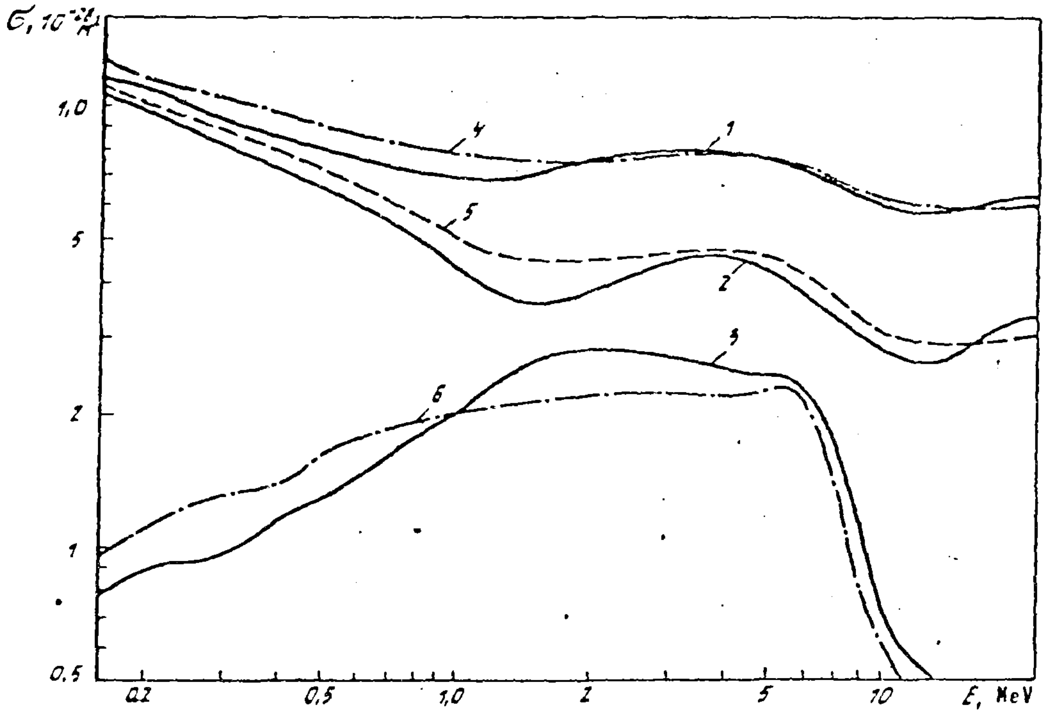

Fig. 4.5. Total cross-section (1) and elastic (2) and inelastic (3) scattering cross-sections in the energy range 0.16-20 MeV as evaluated in the present work and their comparison with the ENDF/B-V evaluation: 4 - σ_t; 5 - σ_n; 6 - $\sigma_{nn'}$

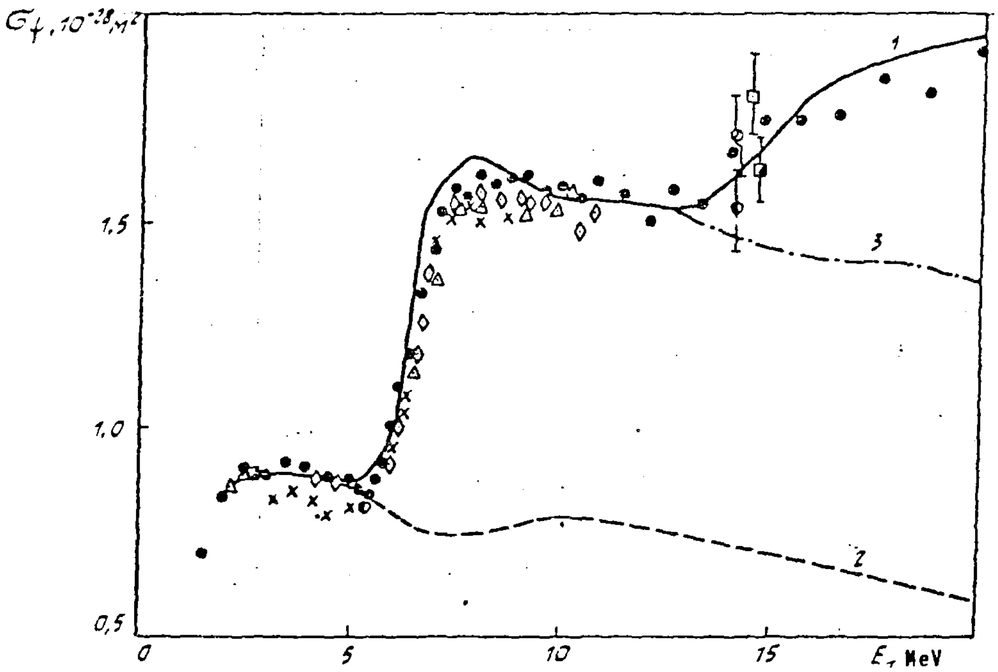

Fig. 5.1. Comparison of calculated and experimental data for fission cross-section in the 2-20 MeV range: 1 - calculation of σ_{nF} ; 2 - σ_{nf} ; 3 - $\sigma_{nf} + \sigma_{nn'f}$ (for notation see Figs 3.1-3.5).

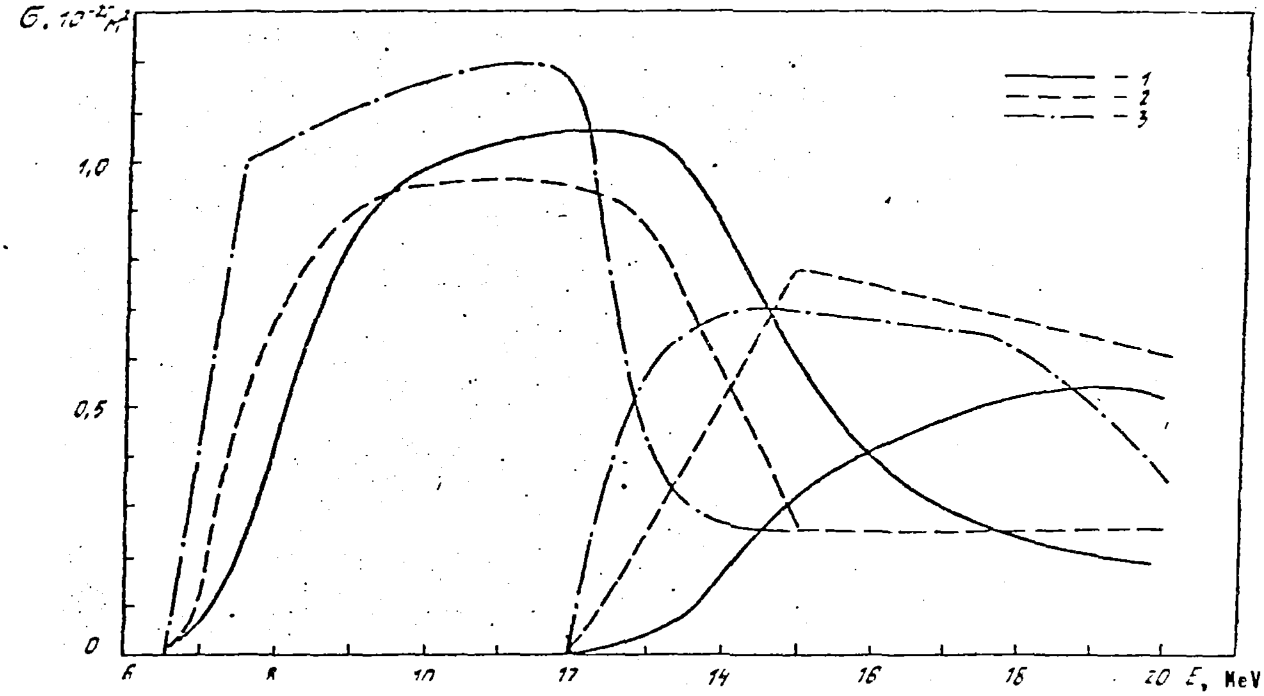

Fig. 5.2. Evaluated figures for cross-sections for the $(n, 2n)$ & $(n, 3n)$ reactions:
1 - present evaluation; 2 - ENDF/B-V evaluation [63]; 3 - ENDL-78 evaluation [64].

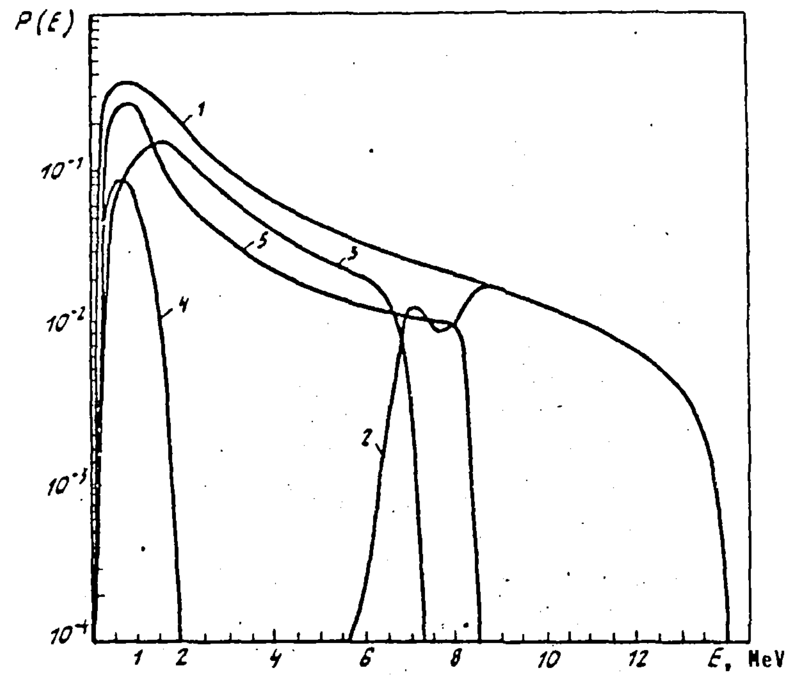

Fig. 6.1. Energy distributions for the first neutrons of reactions: I - $(n, n'x)$; 2 - (n, n'); 3 - $(n, 2n)$; 4 - $(n, 3n)$ at an incident neutron energy of 14 MeV. The spectrum integrals are normalized to the proportions of the corresponding reactions in the (n,n'x) reaction.

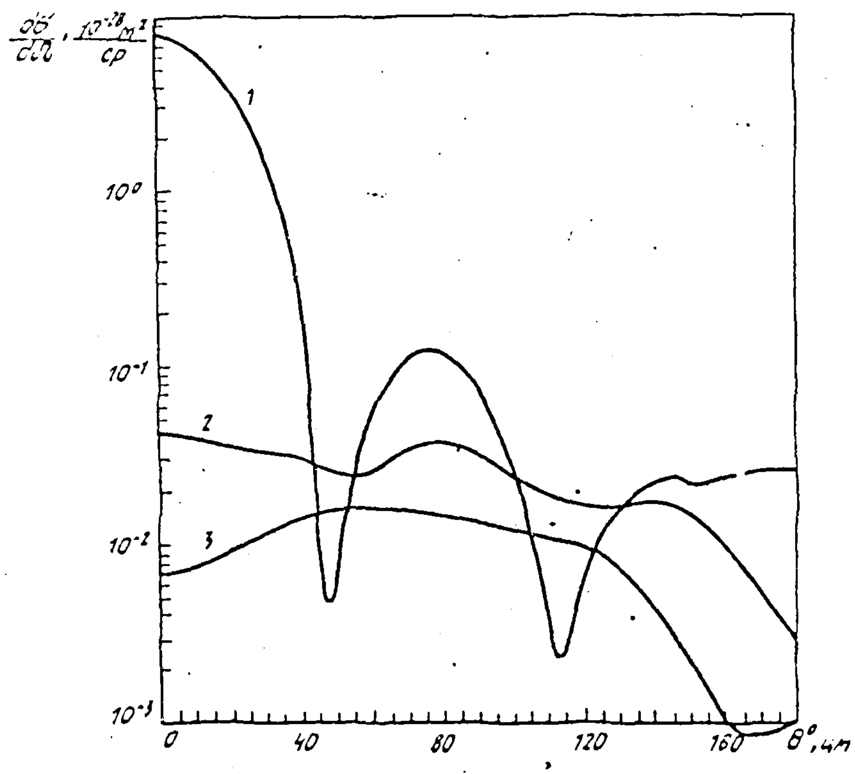

Fig. 6.2. Angular distributions of elastically (1) and inelastically scattered neutrons at levels 2^+ (2) and 4^+ (3) at an incident neutron energy of 4 MeV.

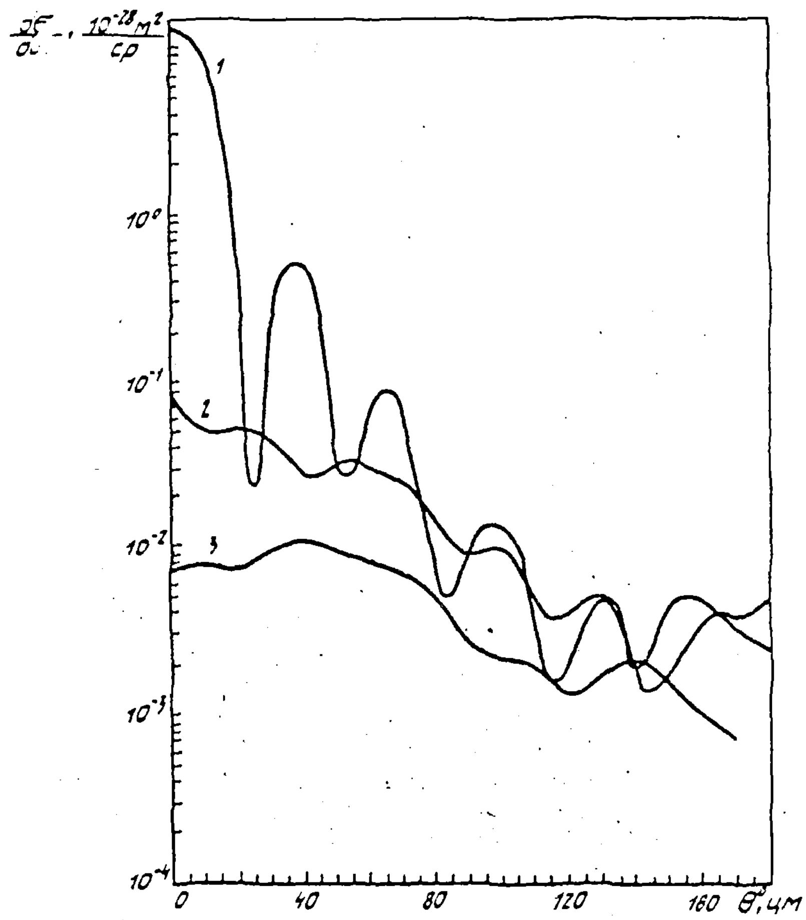

Fig. 6.3. Angular distributions of scattered neutrons at an energy of 14 MeV (for notation see Fig. 6.2).